

Chapter 2

Kinetics of the Interaction of Peptidases with Substrates and Modifiers

Antonio Baici, Marko Novinec, and Brigita Lenarčič

2.1 Introduction

A significant proportion of past and present research on peptidases was/is dedicated to the interactions between enzymes, substrates and modifiers, many of which have a direct bearing to human health. Any study of the efficacy of modifiers aimed at modulating the activity of peptidases begins *in vitro*, for practical reasons using synthetic substrates, which after hydrolysis of a susceptible peptide bond produce a measurable signal proportional to the concentration of hydrolyzed substrate. Enzyme kinetics provides the tools to accomplish this task, which aims at elucidating the underlying kinetic mechanisms of action. This information is necessary when formulating hypotheses on the mechanisms of action of the peptidases with naturally occurring substrates and modifiers, as well with synthetic or semisynthetic modifiers intended to be used as drugs.

The kinetic tools for characterizing substrate turnover by peptidase and interactions with inhibitors and activators are dispersed between numerous specialized publications. Often, important kinetic methods are part of studies whose emphasis is placed on the biological properties of the enzymes and the ‘technical’ part is overlooked. In other instances, kinetic theories are published in journals with predominantly theoretical character and are overlooked as well. Particular methods that are not treated in specialized books can be found in the specific literature. Yet, finding these methods and putting them to work is a responsibility left to the end user. In this chapter, enzyme kinetic concepts relevant to peptidases will be discussed, while general theories can be found in excellent books dedicated to this topic (Cornish-Bowden 2004; Fersht 1977; Segel 1975).

A. Baici (✉)

Department of Biochemistry, University of Zurich, 8057 Zurich, Switzerland

e-mail: abaici@bioc.uzh.ch

M. Novinec • B. Lenarčič

Department of Chemistry and Biochemistry, University of Ljubljana, 1000 Ljubljana, Slovenia

e-mail: marko.novinec@fkkt.uni-lj.si; Brigita.Lenarcic@fkkt.uni-lj.si

2.2 Symbols, Nomenclature, Conventions and Software Used

In the interest of unambiguous communication in research and teaching, especially in reporting results for publication, a consistent use of nomenclature and symbols in enzyme kinetics is highly recommended. We follow here the recommendations of the Nomenclature Committee of the International Union of Biochemistry (International Union of Biochemistry 1979, 1982). Recommended and other symbols are summarized in Table 2.1.

GraphPad Prism version 5.04 for Windows, GraphPad Software (San Diego, California, USA) was used for regression analysis and graphical representations. Numerical simulations of time-dependent processes were performed with Matlab® and Simulink® (MathWorks, Natick, Massachusetts, USA). Model fitting by a combination of numerical simulation and non-linear regression was performed with KinTek Explorer 2.5 software (KinTek Corporation, Austin, Texas, USA). The examples of kinetic experiments shown in this chapter are either unpublished originals from the laboratories of the authors or were provided by colleagues as acknowledged in the figure legends.

2.3 Kinetics of Enzyme-Catalyzed Peptide Bond Hydrolysis

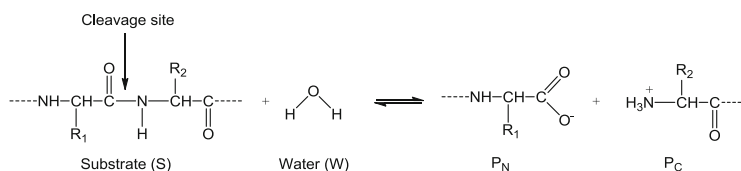
The peptide bond hydrolases or *peptidases* (EC 3.4.x.y) are subdivided into seven catalytic types according to their catalytic mechanism in aspartic, cysteine, glutamic, metallo, asparagine, serine and threonine peptidases (Rawlings et al. 2010). These enzymes catalyze the hydrolytic cleavage of peptide bonds in proteins and peptides of various sizes down to dipeptides using diverse chemical approaches for performing this task at the molecular level. Though, all peptidases share a common catalytic strategy which consists of a proton carrier for delivering the proton from an attacking nucleophile to the leaving group of the peptide being cleaved. In this process, shown in Scheme 2.1, the peptide substrate (S) reacts with water (W) to generate two products, P_N and P_C , which denote the N-terminal and the C-terminal peptide products with respect to the cleaved bond. Only the residues R_1 and R_2 pertaining to the scissile peptide bond are shown in Scheme 2.1. These represent the P_1 and P_1' amino acid side chains of the substrate that bind to the S_1 and S_1' pockets of the enzyme, respectively (Schechter and Berger 1967).

Therefore, the reaction mechanism of peptide bond hydrolysis involves two substrates and two products. The sequence of kinetic events in serine, threonine and cysteine peptidases is shown in Scheme 2.2a in Cleland's notation (Cleland 1963). Without entering the details of the mechanism at the molecular and atomic level, the enzyme binds first the (poly)peptide, a covalently modified enzyme is formed and one of the two products, i.e. the C-terminal part of the original substrate, is released (Polgár 2004a, b). Next, water reacts as the second substrate with the

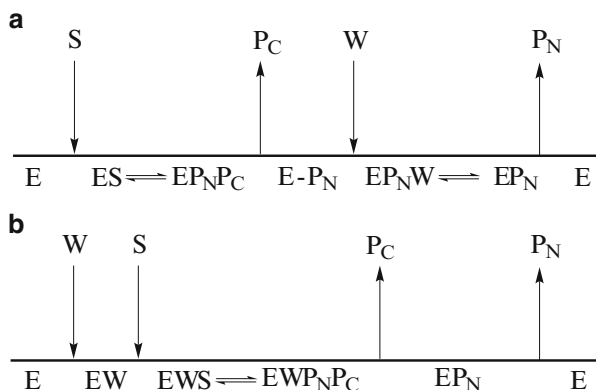
Table 2.1 Symbols for enzyme kinetics

Symbol	Meaning
E	Enzyme
EI, EX	Adsorptive enzyme-inhibitor, enzyme-modifier complex
E-I, E-X	Reversible enzyme-inhibitor, enzyme-modifier X complex
E-I	Inactivated enzyme (irreversible inhibition by covalent interaction)
ES	Enzyme-substrate adsorptive complex (Michaelis complex)
I	Reversible inhibitor or inactivator (=irreversible inhibitor)
k_{cat}	Catalytic constant. Unit: s^{-1}
K_{m}	Michaelis constant. Unit: M
$k_{\text{cat}}/K_{\text{m}}$	Specificity constant. Units: $\text{M}^{-1} \text{s}^{-1}$
K_{s}	Dissociation constant of the enzyme-substrate complex. Unit: M
K_{i}	Dissociation constant of the enzyme-inhibitor complex. Unit: M
$k_{\text{n}}, k_{-\text{n}}$	Rate constants for the n^{th} step of enzyme-catalyzed reactions, positive in the forward and negative in the reverse reaction. Units: $\text{M}^{-1} \text{s}^{-1}$ for second-order, s^{-1} for first-order
P	Product, symbolically also for more than one product
S	Substrate
v	Generic reaction velocity (reaction rate)
v_{i}	Reaction velocity in presence of inhibitors or inactivators
v_{x}	Reaction velocity in presence of a modifier X
v_{s}	Reaction velocity at steady-state
v_{z}	Reaction velocity at the beginning of a reaction (z = zero time)
v_0	Reaction velocity in the absence of modifiers. The index is ‘zero’, not the letter ‘o’
v_{∞}	Reaction velocity following the exponential phase in temporary inactivation
V	Limiting rate, recommended symbol for ‘maximum velocity’ V_{max} . Units: M s^{-1}
X	Generic modifier
λ	First-order rate constant of an exponential process. Unit: s^{-1}
σ	$[\text{S}]/K_{\text{m}}$, dimensionless
t	Time, whose unit will always be the second (s)

The concentration of any species, indicated by a letter enclosed in square brackets has dimensions of $\text{mol dm}^{-3} = \text{M}$. Without additional specification it indicates the concentration of the free species, i.e. not bound to other species. For instance, $[\text{S}]$ = free substrate concentration, $[\text{E}]_{\text{t}}$ = total enzyme concentration

**Scheme 2.1** Peptide bond hydrolysis

modified enzyme whereby the second product, the N-terminal part of the substrate, is released and the enzyme is restored to its original state. This mechanism is known as substituted-enzyme, double-displacement or Ping Pong Bi Bi mechanism. In aspartic peptidases the nucleophile is a water molecule coordinated by the carboxyl groups of two aspartate residues (James 2004). Following substrate binding



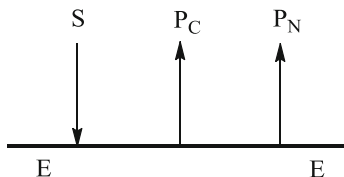
Scheme 2.2 Kinetic mechanisms of peptidases. (a) Serine, threonine and cysteine peptidases; (b) aspartic and metallo peptidases

(Scheme 2.2b), a tetrahedral intermediate is formed, followed by release of the two cleavage products in the same order of Scheme 2.2a. Also in the metallo-peptidases the nucleophile is water, which is bound to a zinc ion, and the mechanism can be sketched (only kinetically) as shown in Scheme 2.2b despite of chemical events differing from those of the aspartic peptidases (Auld 2004; Tallant et al. 2010). For example, in the carboxypeptidase A mechanism the C-terminal product is cleaved off the substrate but retains a salt bridge to a glutamic acid residue until the N-terminal product has left the active center of the enzyme and another water molecule has been bound by the zinc ion. The kinetic mechanism of aspartic and metallopeptidases is therefore of an ordered type.

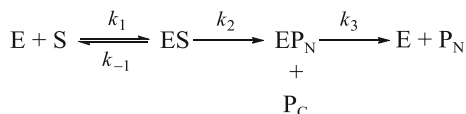
Since water is in great excess, the mechanisms in Scheme 2.2 can be reduced to that in Scheme 2.3 as an ordered Uni Bi mechanism in Cleland's nomenclature, in which water is only formally omitted (Cleland 1963).

In the notation of enzyme kinetics, which includes kinetic constants, Scheme 2.3 is written as shown in Scheme 2.4. Here a further simplification was tacitly introduced by making the reverse reactions of the second and third steps irreversible. Without ignoring the principle of microscopic reversibility, in hydrolytic enzymes this is justified after considering the exergonic character of peptide bond hydrolysis, the high energy barrier of the reverse reaction and the presence of excess water. Again for practical reasons, the mechanism in Scheme 2.4 is often written in the oversimplified form shown in Scheme 2.5, where the second and third steps of Scheme 2.4 are taken together in an apparently single step with the kinetic constant k_{cat} . This corresponds, only formally, to a Briggs-Haldane mechanism, for which the rate is given by the Michaelis-Menten equation with v as steady-state velocity and $V = k_{\text{cat}}[E]_t$ as limiting rate (Eq. 2.1).

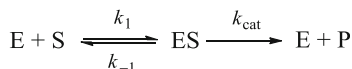
$$v = \frac{V[S]}{K_m + [S]} \quad (2.1)$$



Scheme 2.3 Simplification the peptidase mechanisms to an ordered Uni Bi sequence



Scheme 2.4 Kinetic notation of the simplified ordered Uni Bi mechanism



Scheme 2.5 Short form of the peptidolytic reaction as Uni Uni mechanism

The catalytic and the Michaelis constants for the mechanism in Scheme 2.4 and Eq. (2.1) are given by

$$k_{\text{cat}} = \frac{k_2 k_3}{k_2 + k_3}; \quad K_m = \frac{k_3(k_{-1} + k_2)}{k_1(k_2 + k_3)}. \quad (2.2)$$

Keeping in mind the significance of the last simplification, we will continue the treatment of the kinetics of peptidase action using this formalism including also modifiers such as inhibitors and activators.

2.4 Basic Tools for Kinetic Data Analysis

In this section, after introducing an indispensable method to assess enzyme stability during kinetic assays, the basic notions of graphical and mathematical analysis of kinetic data are introduced.

2.4.1 Checking Enzyme Stability During Assays

Steady-state measurements of substrate turnover are limited to relatively short times, during which the substrate concentration is assumed to change

insignificantly from its initial value. Letting reactions to proceed to completeness allows exploiting the full information contained in progress curves because the tangent in any point of a curve represents a velocity, which is then evaluated in a broad range of substrate concentrations, i.e. from its initial value towards zero or to a value dictated by thermodynamic equilibrium. Besides the conceptual difference between steady-state and progress curve methods in dealing with changing substrate and modifier concentrations, another significant factor is the time scale of the measurements. Steady-state experiments can be set up to record only a short, ‘initial’ part of the whole reaction, in which the measured signal changes linearly with time. Recording an entire progress curve can however take a considerable time, during which the reactants, but more importantly the enzymes, may be subjected to changes that affect their concentration as active species. The instability of several peptidases after dilution in assay buffers for kinetic measurements is well known. Therefore, any study based on progress curves must first ascertain the stability of the enzyme over the whole measurement time. For this purpose, Selwyn developed a straightforward method, which consists in measuring the time course of the reaction under consideration keeping all conditions identical but at two or more enzyme concentrations (Selwyn 1965). The underlying principle is based on the following general form of the rate for any enzyme-catalyzed reaction

$$\frac{d[P]}{dt} = [E] \cdot f\{[S], [X], [P]\}, \quad (2.3)$$

with integral given by

$$[E] \cdot t = f\{[P]\}. \quad (2.4)$$

The analytical form of this integrated equation depends on the particular system but, independently of its complexity, the product concentration $[P]$ only depends on the enzyme concentration multiplied by time. This property is understood intuitively by considering that doubling the concentration of enzyme, i.e. the catalyst, the reaction rate doubles. Thus, for instance, the amount of product generated by an enzyme concentration $[E] = 10 \text{ nM}$ at $t = 120 \text{ s}$ will be the same as with $[E] = 20 \text{ nM}$ and $t = 60 \text{ s}$. Accordingly, a series of progress curves measured at several different values of the enzyme concentration, while keeping all other variables constant, produces a single trace in a plot of $[P]$ versus $[E] \cdot t$ if the enzyme concentration remains constant during the measuring time. If, conversely, the enzyme is denatured or its concentration changes for any other cause, $[E]$ becomes a function of time and plotting $[P]$ versus $[E] \cdot t$ generates as many different curves as the different initial enzyme concentrations used for collecting data. The Selwyn method is illustrated in Fig. 2.1 for testing the suitability of assays lasting a relatively long time in the case of enzyme instability during the assay time (elastase-2) and in the case of enzyme stability (HIV-1 retropepsin). The example with elastase-2 clearly shows that the conditions are inadequate for performing assays over the time indicated, while the assay for HIV-1 retropepsin is appropriate.

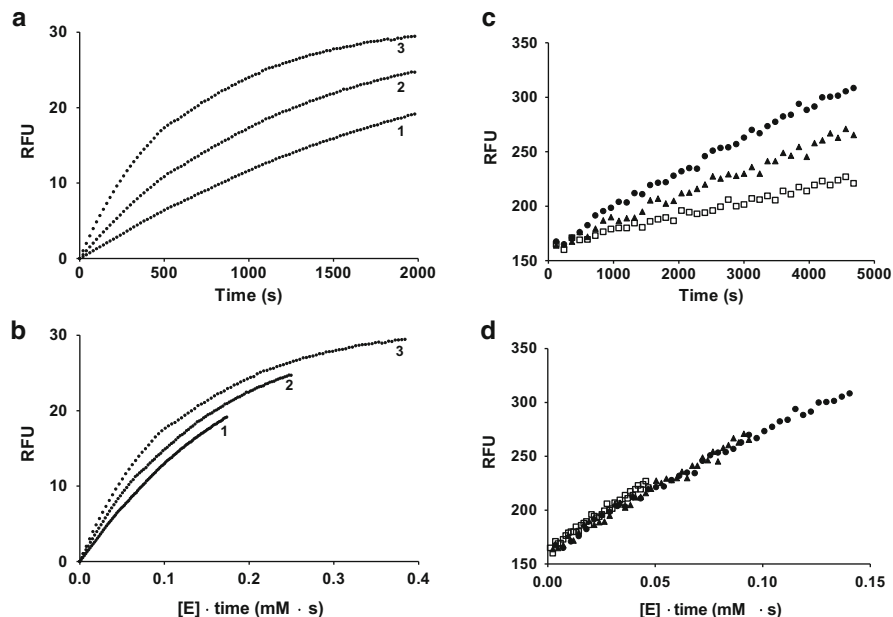


Fig. 2.1 The Selwyn test as a diagnostic tool for time-dependent loss of enzyme activity in continuous assays. (a) and (b): human elastase-2 (leukocyte elastase, EC 3.4.21.37) with 520 μ M MeOSuc-Ala-Ala-Pro-Val-7-(4-methyl)coumarylamide as substrate in 50 mM Tris/HCl buffer, 150 mM NaCl, pH = 7.50, 25 °C; the enzyme concentrations in the assays were 88, 126 and 194 nM in traces 1, 2, and 3, respectively. (c) and (d): Q7K mutant of HIV-1 retropepsin (HIV-1 protease, EC 3.4.23.16) with 10 μ M DABCYL-g-Abu-Ser-Gln-Asn-Tyr-Pro-Ile-Val-Gln-EDANS as substrate. The buffer was 50 mM sodium acetate, 1 mM EDTA, 2.5 mM DTT, 1 M NaCl, 2.5 % glycerol (v/v), 10 % DMSO (v/v), 0.1 % nonidet P-40 (v/v), pH = 4.7, 25 °C. Enzyme concentrations (nM): squares 10, triangles 20, circles 30. RFU = relative fluorescence units, directly proportional to product concentration. Data kindly provided by Dr. H. Roschitzki-Voser and A. Flüttsch, Department of Biochemistry, University of Zurich

2.4.2 Graphical Analysis

Graphical methods were the first to be utilized to extract kinetic information from experiments, while statistical procedures were developed in more recent times and gained popularity after the appearance of commercial software which integrates mathematical methods and drawing facilities. Instead of being obsolete, graphical analysis of kinetic data is very useful for the preliminary screening of experimental results with the aim of identifying a mechanism, or a limited number of mechanisms, and of obtaining approximate values of kinetic parameters, which can be further used for final refinement by mathematical methods. Since curved plots cannot be used for ‘manual’ calculations, the original rate equations must first be linearized using a variety of algebraic manipulations. The slopes of straight lines can thus be calculated and useful intercepts with the Cartesian coordinates can be

guessed directly or by extrapolation. The subjectivity in drawing straight lines through experimental points, which are affected by inevitable errors, can in principle be overcome by linear regression procedures. However, their applicability is subject to mathematical rules that cannot be ignored, particularly concerning error structure and distribution (see below). If these rules are ignored, the calculated kinetic parameters make little sense because their statistical significance cannot be guessed. This poses limitations in reporting reliable results for publication as well as for the purposes of good manufacturing practice and good laboratory practice, notably in pharmaceutical sciences.

2.4.3 Regression Analysis

Linear and non-linear regression methods are widely used in enzyme kinetics. A thorough review of the basics of regression analysis, which belongs to the group of parametric statistical methods, has been published by Johansen and Lumry (1961). The authors put emphasis on kinetic applications and pointed out the importance of knowing the structure and distribution of experimental errors as a prerequisite for the applicability of regression analysis. Before utilizing any regression procedure the following criteria must be satisfied (pp. 355–356 in Cornish-Bowden 2004):

- The errors are normally distributed, i.e. distributed according to a bell-shaped Gauss-curve.
- The variance of the independent variable is zero, i.e. there are only errors in the dependent variable. For instance, in Michaelis-Menten kinetics $[S]$ is assumed to be error-free while errors are associated with the rate v .
- The weight of the errors is known.
- The value and sign of a given error is not related to the values and signs of other errors. In mathematical language: the errors are stochastically independent from each other.¹
- Systematic errors can be neglected, i.e. the distribution curve of each error has the mean value zero. In practice, we have no doubts that we are using the correct equation.

Unfortunately and recurrently, these mathematical requirements are disregarded. Unlike linear regression, which goes straight to calculating the best fit of slope and intercept in a set of data that describe a linear dependence of the variables using the least-squares approach, non-linear regression requires initial estimates of the parameters. These are used in an iterative procedure until a minimum is reached for the sum of the squared deviations.

¹ Stochastics, ‘the art of guessing’ (Greek *stóchos* = guess), comprises the mathematical theories of probability and statistics. If the happening of an event is not influenced by the happening of another event the two events occur at random and are said to be stochastically independent.

The precision of the best-fit values obtained by non-linear regression analysis is typically reported as the standard errors derived during the regression procedure and are based on the covariance matrix. The values of the standard errors are used to compute confidence intervals, which represent a better criterion to judge the goodness of fit. Thus, if calculations are performed with software that computes confidence intervals, these should be included in reporting results since standard errors may unacceptably underestimate the real errors if the parameters are not well constrained by data. In any case, analysis of the mutual dependency of all estimated parameters is essential, even if small values of the standard errors would suggest an excellent fit. With equations containing two or more parameters it can happen that their values calculated by non-linear regression are not unique, meaning that another set of parameters would ‘nicely’ fit data as well. Also, one or more parameters may be redundant, suggesting that a simpler model would better describe the data. Software packages, such as for instance GraphPad Prism, parameter dependency is calculated as part of goodness of fit assessment. See also the comments on FitSpace for the Global Kinetic Explorer in Sect. 2.4.4.

The adherence to or deviation of fitted curves from a model can be assessed by methods that are part of commercial software, such as GraphPad Prism. These include residual analysis and the runs test. Residuals are the vertical distances between experimental points and the fitted curve and may be positive or negative. Any non-random, i.e. systematic distribution of the residuals, should be carefully examined and the fit procedure repeated with alternative models. A ‘run’ is defined as a sequence of points, which are located either above or below the best fit curve calculated by regression analysis. If the model produces a poor fit to data, clusters of points either above or below the curve are observed and the total number of expected runs, which can be calculated, is smaller than that expected from randomly distributed errors.

A comment to a frequent flaw in describing the application of regression analysis, which is not merely a semantic issue, is required at this stage. In the literature, sentences like the following are typically found: ‘... data were fitted to equation X’, or ‘... parameters shown in Table Y were obtained by fitting experimental results to equation Z’. These expressions suggest that the available data were manipulated until they reached the desired fit to a model. The correct sentences should read instead: ‘... equation X was fitted to data’, and ‘... equation Z was fitted to experimental results to calculate the parameters shown in Table Y’.

2.4.4 Numerical Integration and Global Fit of Progress Curves

Non-linear regression is based on the fulfillment of the criteria discussed in the preceding section. Moreover, integrated rate equations and their utilization in non-linear regression procedures are often based on restrictive assumptions that

can or cannot be satisfied experimentally. Also, in many instances analytical integrals of rate equations do not exist at all. In such cases computational limitations can be overcome by performing numerical instead of analytical integration of rate equations. This procedure supplies a value of the area under a curve with an approximation that depends on the algorithm chosen and supplies an almost exact solution. One or more differential equations can be integrated numerically at the same time to produce simulated concentration vs. time profiles. Such curves, generated with initial guesses of the parameters of the considered equations, can be compared with experimental data, the squared differences between them can be calculated, and this procedure can be iterated until reaching a minimum of the squared deviations. The algorithms to perform the necessary calculations by numerical methods (solvers) have been implemented in several software packages, of which just two are commented here. Simulink[®] operates within the numerical computing software MATLAB^{®2} and offers block libraries that are used to represent symbolically time-dependent processes. Eight solvers with fixed or variable step size are available to cover a broad band of applications in any field of physics, chemistry and engineering that requires numerical integration of differential equations of nonstiff and stiff problems (for a stiff differential equation some numerical methods for its solution are unstable unless the step size used for integration is very small). Simulink is a valuable tool for educational purposes in enzyme kinetics because it offers a friendly working interface and compels the user to put hands on by planning and programming the whole numerical integration procedure, from writing differential equations based on a kinetic model to making connections between kinetic paths in even very complex mechanisms. Simulink can also be used to perform parameter optimization by combining numerical integration and non-linear regression. Unfortunately, two major drawbacks are slow performance using conventional desktop computers and the lack of statistical information of the best-fit parameters, such as standard errors and confidence intervals.

A software package fully dedicated to enzyme kinetics is the KinTek Global Kinetic Explorer³ (Johnson 2009; Johnson et al. 2009a, b). KinTek does not require particular efforts from the part of the user and kinetic models are entered with letters connected by the = sign. The necessary differential equations are set up and all rate constants for forward and reverse reaction directions are displayed automatically. A graphical user interface allows scrolling the values of the parameters to be calculated and to directly visualize the results on screen in real time. This is particularly useful for guessing the initial values that are necessary for the fitting procedure. After entering experimental data, which can either be single curves or sets of curves and even different sets of experiments, simulation is performed by numerical integration. The curve resulting from numerical integration is compared with the experimental curve and the sum of the squared deviations is calculated. The procedure is iterated until a minimum is reached. The strongest feature of

² <http://www.mathworks.com>

³ <http://www.kintek-corp.com/KGExplorer>

KinTek is the FitSpace Explorer, which ‘calculates the dependence of the sum square error on each pair of parameters while allowing all remaining parameters to be adjusted in seeking the best fit’. Results are displayed graphically as three-dimensional plots, which reveal all relationships between parameters and show whether the set of fitted parameters is unique and well constrained by the data.

2.5 Calculation of k_{cat} and K_{m}

Low molecular mass peptide substrates carrying fluorogenic or chromogenic leaving groups, or containing internally quenched fluorescent moieties, are typically used to evaluate the ability of peptidases to catalyze the cleavage of peptide bonds. Among the purposes of this investigation are the determination of substrate specificity and the identification of adequate substrates for assessing the action of modifiers *in vitro*. To accomplish these tasks it is necessary to determine the kinetic parameters k_{cat} and K_{m} either individually, from which their ratio can then be calculated, or $k_{\text{cat}}/K_{\text{m}}$ can be measured directly. It is superfluous to mention that such measurements should be carried out as precisely as possible using the most appropriate methods. The ratio $k_{\text{cat}}/K_{\text{m}}$, referred to as the ‘specificity constant’ (Fersht 1977), is the parameter of choice for assessing the competence of an enzyme in performing catalysis preferentially on a given substrate in the presence of others (pp. 36–39 in Cornish-Bowden 2004). The ratio $k_{\text{cat}}/K_{\text{m}}$, which has also been called ‘catalytic efficiency’, ‘catalytic potential’ and ‘performance constant’, is a misleading parameter if used to compare the catalytic effectiveness of two enzymes on the same substrate (Eisenthal et al. 2007; Koshland 2002).

2.5.1 Graphical Analysis

The direct linear plot created by Eisenthal and Cornish-Bowden (Cornish-Bowden and Eisenthal 1974; Eisenthal and Cornish-Bowden 1974) is undoubtedly the most robust and trustworthy among other graphical procedures for calculating the kinetic parameters of substrate turnover by enzymes (Sect. 2.6 in Cornish-Bowden 2004). In this method, the Michaelis-Menten equation (2.1) is rearranged by considering K_{m} and V as variables and the measured v values and known substrate concentrations $[S]$ as constants

$$V = v + \frac{v}{[S]} K_{\text{m}}. \quad (2.5)$$

The straight lines described by Eq. (2.5) have v as ordinate intercept and $v/[s]$ as slope in the parameter space defined by V and K_{m} . In the absence of errors, the direct linear plot consists of a sheaf of straight lines intersecting at a common point,

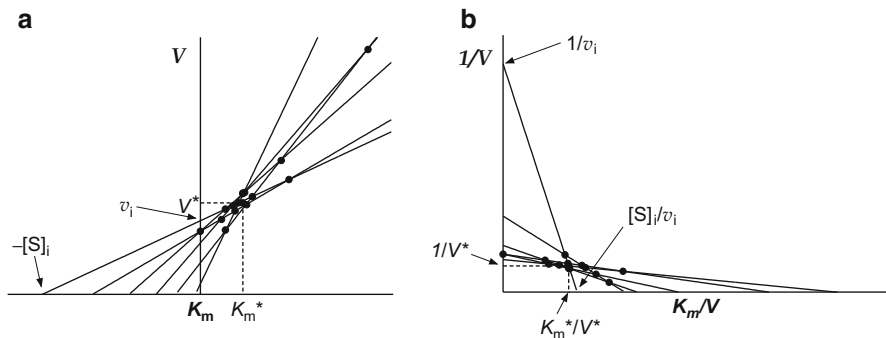


Fig. 2.2 The direct linear plot. The same observations were plotted in the original form (a) and in the reciprocal variant (b). In both cases the maximum number of intercepts for n observations is given by $n(n - 1)/2$. In panel (a) the best estimates of the parameters V and K_m , denoted by an *asterisk*, are obtained by reading out the coordinates of the median of the intersections on the axes of the diagram. Similarly in panel (b) the best estimates of $1/V$ and K_m/V are denoted by *asterisks* and determined from the coordinates of the median of all intersections (*dots*), from which the parameters are calculated

while with experimental data multiple intersection points result from inevitable errors. The maximum number of intersections is $n(n - 1)/2$, where n is the number of observations. The direct linear plot belongs to the group of distribution-free or non-parametric statistical methods. With respect to parametric methods, for whose correct application normally distributed errors are a prerequisite, non-parametric approaches do not depend on error distribution. For this property, distribution-free methods are less sensitive to the presence of outliers. While parametric statistics considers the sample mean as the best-fit, distribution-free methods make use of the median as the best estimator. This value can be visually identified by sorting all numbers under consideration in increasing order and taking the figure which lies in the middle of the series. For an odd number of data the median is placed ‘in the middle’ and for an even number of data the median is calculated as the mean of the two ‘central’ values.

In the ideal case, intersections occur in the first quadrant as in the representation of Fig. 2.2a. Negative estimates of V and/or K_m may be observed when any intersection of the lines occurs in the second or third quadrant. Second quadrant intercepts are treated as they would occur at face value (i.e. the abscissa coordinate is multiplied by -1) and third quadrant intercepts are considered as being both large and positive. This problem can be fixed considering a practical variant of the direct linear plot, which consists in drawing straight lines from intercepts $[S]_i/v_i$ and $1/v_i$ instead of $-[S]_i$ and v_i (Fig. 2.2b) (Cornish-Bowden and Eisenthal 1978). With this alternative method the intersections can be identified easier than in the original plot and any intersection in the second or third quadrant does not need a particular treatment.

Since both variants of this plot become crowded with increasing number of data, it is possible to skip the graphical representation and to calculate instead the intersections analytically. This is easily accomplished with the aid of a spreadsheet calculation program, which can be programmed to solve n systems of pairs of linear equations from n measurements and to show the medians of all intersections for both axes. Confidence intervals of the median can be estimated from the ranked intersections to show the statistical significance of the measurements (Cornish-Bowden et al. 1978).

2.5.2 Non-linear Regression Analysis

The Michaelis-Menten equation is a friendly one, since initial estimates are easily calculated from data, e.g. by taking the largest value of the measured velocities as an estimate of V and the median of the substrate concentrations to estimate K_m . The example in Fig. 2.3 shows the fit of Eq. (2.1) to a set of measurements for evaluating V and K_m for a substrate of bovine α -chymotrypsin. The figure shows the best fit curve and the 95 % confidence band considering equal weights for all data points. The fit by non-linear regression was also performed using the ‘automatic outlier elimination’ option of GraphPad Prism with results listed for comparison in Table 2.2. The same data were also evaluated with the direct linear plot (Sect. 2.5.1), with the appropriate 95 % confidence intervals (Cornish-Bowden et al. 1978). Inspection of the best fit values obtained by the three methods shows that the apparent ‘outlier’, i.e. the point outside the 95 % confidence band in Fig. 2.3, has a larger impact on K_m than on V , with the larger discrepancy between ordinary regression and outlier elimination. Automatic outlier elimination should be used with caution, especially because such eliminations may be rather arbitrary.

Another variant is robust non-linear regression, which is based on a Lorentzian instead on Gaussian distribution of errors and makes the fit less sensitive to outliers. At least as implemented by GraphPad Prism, this is however a qualitative method to assess the effect of possible outliers without generating standard errors and confidence intervals. This method applied to the data in Fig. 2.3 gave in any case $V = 0.137$ ($\mu\text{M s}^{-1}$) and $K_m = 30.8$ μM , which are very close to the values obtained with the direct linear plot.

When the k_{cat}/K_m ratio needs to be calculated from the individual values of the two parameters together with their standard errors (SE) or standard deviations (SD), the SE or SD associated with k_{cat}/K_m can be calculated with the Fenner formula (Fenner 1931)

$$\frac{\bar{x}_1 \pm s_{\bar{x}_1}}{\bar{x}_2 \pm s_{\bar{x}_2}} = \frac{\bar{x}_1}{\bar{x}_2} \pm \frac{1}{\bar{x}_2^2} \sqrt{\bar{x}_1^2 s_{\bar{x}_2}^2 + \bar{x}_2^2 s_{\bar{x}_1}^2}, \quad (2.6)$$

where $\bar{x}_i \pm s_{\bar{x}_i}$ indicate the means with their associated ‘errors’. In the same paper Fenner also described how to calculate the errors of sums, subtractions

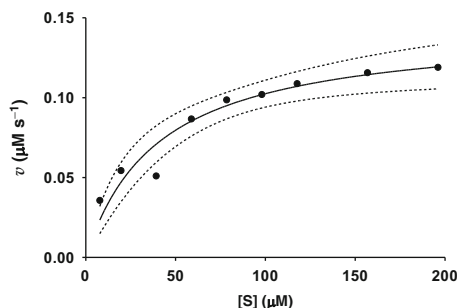


Fig. 2.3 Fit of the Michaelis-Menten equation (2.1) to data by non-linear regression. The *solid line* represents the best fit and the *dashed lines* show the 95 % confidence band. Measurements performed with bovine α -chymotrypsin and N-succinyl-Ala-Ala-Pro-Phe-p-nitroanilide as substrate in 0.1 M Tris/HCl buffer, pH = 7.80, 25 °C. The α -chymotrypsin active site concentration was determined by burst kinetics and the enzyme concentration in the assay was 2.8 nM

Table 2.2 Comparison of kinetic parameters for the data in Fig. 2.3 calculated by non-linear regression fit of Eq. (2.1) to data and with the direct linear plot

	V ($\mu\text{M s}^{-1}$)	K_m (μM)
NLR	0.144 ± 0.013 (0.114–0.174)	40.3 ± 11.2 (13.9–66.7)
NLR, outlier elim.	0.134 ± 0.004 (0.125–0.143)	27.6 ± 3.0 (20.2–34.9)
Direct linear plot	0.138 (0.127–0.149)	31.0 (20.9–44.8)

The \pm values represent standard errors from regression analysis and those in parentheses correspond to 95 % confidence intervals

NLR non-linear regression, *outlier elim.* automatic outlier elimination

and multiplications of mean values with associated errors. For example, from $k_{\text{cat}} = 14.7 \pm 0.7 \text{ s}^{-1}$ and $K_m = (95 \pm 4) \times 10^{-6} \text{ M}$ the ratio of the two parameters is calculated as $k_{\text{cat}}/K_m = 154\,737 \pm 9\,836 \text{ M}^{-1} \text{ s}^{-1}$. For publication purposes, this last value would be conveniently rounded up e.g. as $154\,700 \pm 9\,800 \text{ M}^{-1} \text{ s}^{-1}$.

2.5.3 First-Order Kinetics

In some instances the substrates of peptidases, such as proteins with a large molecular mass, are not amenable to large excursions in their concentrations for calculating kinetic parameters by any of the methods illustrated in this section. Equation (2.1) reduces to a first-order equation if $[S] \ll K_m$, with the first-order rate constant V/K_m , and to a zero-order equation for $[S] \gg K_m$, with $v = V$. First-order kinetics can thus be exploited for the direct calculation of V/K_m from experiments performed at low substrate concentrations. An illustrative example is the degradation of the four human IgG subclasses, named IgG1 to IgG4, by elastase-2 (human leukocyte elastase, EC 3.4.21.37) into discrete fragments (Baici et al. 1980).

Following incubation of monoclonal IgGs with elastase-2 for various times, the fragments were separated by denaturing polyacrylamide gel electrophoresis, the bands on the gel were identified by immunochemistry and their intensities, proportional to concentrations, were determined by gel scanner densitometry. The first enzymatic cleavage of IgG occurred in the hinge region and this represented the primary hydrolytic degradation of the protein, which was followed by other proteolytic events that occurred at slower rates. Thus, following the disappearance of IgG in the first part of reaction progress offers a mean for characterizing the kinetic features of the most susceptible peptide bond. The band intensities for the disappearing IgG-band at various incubation times were plotted and a single exponential was fitted to data to obtain first-order rate constants corresponding to V/K_m . These values, divided by the titrated enzyme active site concentration, gave second-order constants k_{cat}/K_m of 12.3, 4.3, 63.3 and $1.2 \text{ M}^{-1} \text{ s}^{-1}$ for IgG1, IgG2, IgG3 and IgG4, respectively. Considering the limits of the method, these numbers provide a practical semiquantitative criterion for comparing the relative susceptibilities of the IgG subclasses to proteolysis. The same method can be used to characterize the kinetics of limited proteolysis, i.e. a single cut in precursor proteins. Precision can be enhanced by measuring the variation of protein concentration with time e.g. by HPLC.

2.5.4 The Integrated Michaelis-Menten Equation

Equation (2.1) can be integrated to give

$$\frac{[P]}{t} = V + \frac{K_m}{t} \ln \left\{ 1 - \frac{[P]}{[S]_t} \right\}, \quad (2.7)$$

which can be written in different equivalent forms but remains in any case an implicit equation (Orsi and Tipton 1979). Although V and K_m can be calculated as intercept and slope from the straight line obtained in a plot of $[P]/t$ vs. $\ln(1 - [P]/[S]_t)/t$, the procedure cannot give statistically reliable values of the parameters because the errors associated with $[P]$ appear in both the dependent and the independent variable (Johansen and Lumry 1961). Several alternative graphical methods are known that use integrated equations for calculating kinetic parameters including modifiers as well as substrate and product inhibition (Orsi and Tipton 1979), but are subjected to the same statistical limitation. Due to this restriction, the use of the integrated Michaelis-Menten equation instead of another approach for calculating statistically valid kinetic parameters remains a matter of taste. In general however, progress curves contain much more information than initial velocity measurements and exploiting the entire course of enzymatic reactions depends on how the progress curves are treated for quantitative purposes, e.g. using numerical integration methods and disregarding analytical integration as described in the next subsection.

2.5.5 Numerical Integration of the Differential Equation

As an alternative to analytical integration of the Michaelis-Menten equation, numerical integration can be performed. We illustrate this procedure with an example of human cathepsin K and a synthetic dipeptide substrate. Data were collected as described in the legend of Fig. 2.4 and the Michaelis-Menten equation was fitted by numerical integration combined with non-linear regression using the KinTek Global Kinetic Explorer program. With reference to Scheme 2.5, k_1 was kept fixed at the value of $100 \mu\text{M}^{-1} \text{s}^{-1}$, while k_{cat} and k_{-1} were globally fitted using all traces. During the 500 s of the experiment in panel (b) the assays passed the Selwyn test (Sect. 2.4.1). The global fit to data collected for either 20 or 500 s was not perfect, as shown by the best-fit traces systematically deviating from data for some of the curves. This is a characteristic of global fitting and represents the rule rather than the exception even with high quality data collected as precisely as possible. The issue is that global fitting is not permissive to even small deviations from ideal progress curves, i.e. data should not contain errors and should perfectly adhere to the model. Nevertheless, the best-fit values of the kinetic parameters calculated by globally fitting data in panels (a) and (b) of Fig. 2.4 were similar. The slopes of the curves in panel (a) were used to calculate the kinetic parameters with the direct linear plot (Sect. 2.5.1) and by non-linear regression (Sect. 2.5.2), giving reasonably comparable results as shown in Table 2.3.

A limitation of the application of numerical integration to data as those in Fig. 2.4 is that error estimates cannot be obtained for k_{cat} and K_{m} because the individual rate constants cannot in general be calculated with certainty and they are affected by large standard errors. However, this does not preclude the calculation of good estimates of for k_{cat} and K_{m} because the same values will be obtained by any combination of the parameter sets estimated by numerical integration (Johnson 2009).

2.6 Classical and Tight-Binding Enzyme Modification

Enzyme inhibitors can be divided into two broad types depending on whether the enzyme-inhibitor complex can dissociate back to free enzyme and inhibitor (reversible) or not (irreversible). Irreversible inhibition, in the following called ‘inactivation’, will be treated in Sect. 2.8. Reversible inhibitors can either bind very quickly to enzymes, e.g. as a diffusion controlled process, or it may take a relatively long time to complete the formation of the enzyme-inhibitor complex. Morrison (Morrison 1982) proposed a classification of reversible enzyme inhibitors based on the rate of formation of the E·I complex and on the relative concentrations of enzyme and inhibitor as shown in Table 2.4.

Classical reversible inhibitors rapidly associate and dissociate for $[I]_{\text{t}} > [E]_{\text{t}}$, so that the condition $[I] \approx [I]_{\text{t}}$ could be taken as granted. However, the relative

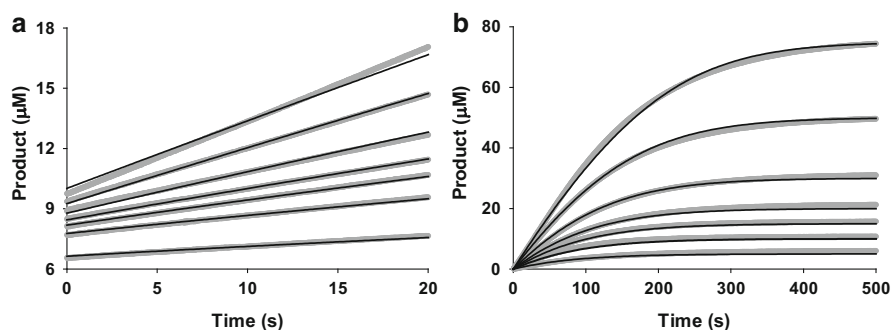


Fig. 2.4 Global fit of reaction progress curves. Human Cathepsin K was rapidly mixed in a stopped-flow apparatus with Z-Phe-Arg-7-(4-methyl)coumarylamide. Two sets of measurements were performed using the same solutions of enzyme and substrate kept in separate syringes with measuring times of 20 s (panel **a**) and 500 s (panel **b**). The concentrations after mixing were: enzyme = 20 nM of titrated active sites, substrate 5, 10, 15, 20, 30, 50 and 75 μM (from *bottom* to *top* traces). 100 mM sodium phosphate buffer, 5 mM dithiothreitol, pH = 6.00, temperature $25 \pm 1^\circ\text{C}$. *Thick traces* represent data and *thin continuous lines* best fit curves

Table 2.3 Comparison of values of the kinetic parameters from the data in Fig. 2.4 calculated by numerical integration of the Michaelis-Menten equation, conventional non-linear regression or with the direct linear plot

	V ($\mu\text{M s}^{-1}$)	K_m (μM)
NI (Fig. 2.4a)	0.57	50.8
NI (Fig. 2.4b)	0.62	48.6
NLR	0.53 ± 0.02 (0.48–0.58)	50.7 ± 4.0 (40.9–60.5)
DLP	0.49 (0.33–0.68)	42.2 (24.6–65.1)

The \pm values represent standard errors from regression analysis and those in parentheses correspond to 95 % confidence intervals

NI numerical integration with KinTek software, NLR non-linear regression, DLP direct linear plot

magnitudes of $[\text{E}]_t$, $[\text{I}]_t$ and K_i are not considered in this classification and a classical inhibitor becomes a tight-binder if the enzyme concentration is raised to the order of magnitude of K_i . For high-affinity modifiers inhibition occurs with $[\text{I}]_t \approx [\text{E}]_t$ at the low enzyme concentrations typically used *in vitro* with $[\text{I}]_t$ in the order of magnitude of its K_i value, so that $[\text{I}]_t \approx [\text{E}]_t \approx K_i$. Thus, Morrison's relationships between $[\text{E}]_t$ and $[\text{I}]_t$ for the tight-binding and the slow, tight-binding classes of inhibitors in Table 2.4, originally formulated as $[\text{I}]_t \approx [\text{E}]_t$, are more coherent by changing them to $[\text{I}]_t \approx [\text{E}]_t$ and K_i . In this section we will deal with the fast acting classes of inhibitors while the slow processes will be discussed in Sects. 2.7 and 2.8.

Enzyme activation can be divided into essential and non-essential. As intuitively indicated by these adjectives, essential activation denotes the compelling presence of an activating partner in order for an enzyme to exert catalysis, while non-essential activation is an elective property of some substances that bind enzymes and enhance thereby their activity over the threshold observed in their absence.

Table 2.4 Classification of reversible enzyme inhibitors [modified after Morrison (1982)]

Type of inhibition	Relationship between $[E]_t$ and $[I]_t$	Rate of formation of the inhibited complex
Classical	$[I]_t \gg [E]_t$	Fast
Tight-binding	$[I]_t \approx [E]_t$ and K_i	Fast
Slow-binding	$[I]_t \gg [E]_t$	Slow
Slow, tight-binding	$[I]_t \approx [E]_t$ and K_i	Slow

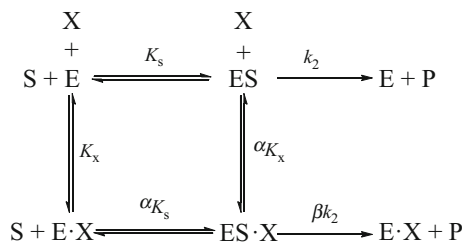
For the tight-binding and the slow, tight-binding cases the original definition $[I]_t \approx [E]_t$ has been changed into $[I]_t \approx [E]_t$ and K_i

2.6.1 The General Modifier Mechanism

When classical inhibitors bind their target enzymes and there is no further product release for $[I] \rightarrow \infty$, enzyme activity is driven to zero and the inhibition is called linear, complete or full. In some instances an ESI-complex exists and is catalytically active, in which case the inhibition is called hyperbolic or partial. The terms ‘linear’ and ‘hyperbolic’ refer to the form of plots of $1/v$ versus $[I]$. Since the name ‘inhibition’ without further specification is generic, the adjectives ‘linear’ or ‘hyperbolic’ as well and the inhibition type (competitive, uncompetitive or mixed) are added.

Non-essential activation is kinetically similar to hyperbolic inhibition, while an essential activator can be seen as a co-substrate. Therefore, classical inhibition and activation can be conveniently described by the general modifier mechanism proposed by Botts and Morales (1953) and treated in a uniform way with a common equation. The general modifier mechanism for unireactant enzymes, and consequently also for peptidases under the conventions discussed in Sect. 2.3, is shown in Scheme 2.6. The ternary ES·X complex between enzyme, substrate and modifier X can be formed through the paths $E \rightarrow ES \rightarrow ES \cdot X$ or $E \rightarrow E \cdot X \rightarrow ES \cdot X$. This is logical because the free energy change of the two paths is the same and thus their overall equilibrium dissociation constant is also the same, i.e. $K_s \alpha K_x = K_x \alpha K_s$ and the scheme represents a thermodynamic box. When Scheme 2.6 is written for an inhibitor, X and K_x may be substituted by I and K_i , respectively, while for an activator these symbols may be changed into A and K_a .

The steady-state rate equation for the general modifier mechanism contains terms in $[S]^2$, $[X]^2$, $[S]^2[X]$ and $[S][X]^2$, which poses limits to its practical application for extracting individual rate constants from experiments. However, assuming that binding of X to E and ES is at quasi-equilibrium, while for the fluxes around ES and ES·X (the catalytic steps) the steady-state assumption is valid, equilibrium dissociation constants can be used in place of individual rate constants as shown in Scheme 2.6 to derive the rate equation, which is given by

**Scheme 2.6** The general modifier mechanism**Table 2.5** Reversible modifier mechanisms as particular cases of the general modifier mechanism

α	β	Modifier mechanism
$\alpha = \infty$	$\beta = 0$	Linear competitive inhibition
$0 < \alpha < \infty$	$\beta = 1$	Hyperbolic competitive inhibition
$\alpha \rightarrow 0, K_x \rightarrow \infty$	$\beta = 0$	Linear uncompetitive inhibition
$0 < \alpha < 1$	$0 < \beta < 1$ and $\alpha = \beta$	Hyperbolic uncompetitive inhibition
$1 \leq \alpha < \infty$	$\beta = 0$	Linear mixed inhibition
$1 \leq \alpha < \infty$	$0 < \beta < 1$	Hyperbolic mixed inhibition
$1 \leq \alpha < \infty$	$\beta > 1$	Non-essential activation
$0 < \alpha < 1$	$0 < \beta$ and $\alpha < \beta$	Hyperbolic mixed inhibition or non-essential activation depending on [S]

$$\frac{v}{V} = \frac{\sigma \left(1 + \beta \frac{[\text{X}]}{\alpha K_x} \right)}{1 + \frac{[\text{X}]}{K_x} + \sigma \left(1 + \frac{[\text{X}]}{\alpha K_x} \right)} \quad (2.8)$$

The symbol σ for $[\text{S}]/K_m$ is used here and in the following for practical reasons. Equation (2.8) applies to classical inhibition types, either linear or hyperbolic, and to activators. The coefficient α specifies the position of the equilibria and the character of the modifier, which for inhibitors can be competitive, uncompetitive or mixed. With $\beta = 0$ inhibitors are linear, with $0 < \beta \leq 1$ inhibitors are hyperbolic, while $\beta > 1$ indicates non-essential activation. Various combinations of the α and β coefficients characterize a large number of diverse reversible modifier mechanisms (Fontes et al. 2000) as shown in Table 2.5. Many such combinations have never been observed for modifiers of peptidases but they may occur for other enzyme classes. For instance, the last row of Table 2.5 contains, among conditions under which only activation is observed, also those that generate either inhibition or activation depending on substrate concentration. Linear uncompetitive inhibition has only purely theoretical character for peptidases but it is considered because, blended with competitive inhibition, it is necessary to describe all gradations of the interesting category of mixed inhibitors. To maintain a consistent nomenclature, for

linear uncompetitive inhibition in Table 2.5 we can figure out that $K_i \rightarrow \infty$ and $\alpha \rightarrow 0$ at the same time, so that αK_i has a finite value, but obviously individual values of α and K_i cannot be measured.

2.6.2 The Specific Velocity Plot

A graphical method for analyzing the kinetics of enzyme modification according to the general modifier mechanism is the specific velocity plot (Baici 1981). The plot is based on the equation

$$\frac{v_0}{v_x} = \frac{[X] \left(\frac{1}{\alpha K_x} - \frac{1}{K_x} \right)}{1 + \beta \frac{[X]}{\alpha K_x}} \frac{\sigma}{1 + \sigma} + \frac{1 + \frac{[X]}{K_x}}{1 + \beta \frac{[X]}{\alpha K_x}}, \quad (2.9)$$

in which the rates in the absence (v_0) and presence of the modifier (v_x) are normalized as a dimensionless ratio, which is a function of the dimensionless ratio $\sigma/(1 + \sigma)$, known as specific velocity. Equation (2.9) is a handy tool that describes any particular case of the general modifier mechanism (Scheme 2.6) as straight lines for inhibitors and activators, provided the quasi-equilibrium assumption is valid. Any consistent deviation from linearity should be considered individually and substrate inhibition, violation of the quasi-equilibrium assumption or others causes evaluated.

The function represented by Eq. (2.9) is defined in the interval $0 < \sigma/(1 + \sigma) < 1$. For $[S] \rightarrow 0$, $\sigma/(1 + \sigma) \rightarrow 0$ and for $[S] \rightarrow \infty$, $\sigma/(1 + \sigma) \rightarrow 1$. When plotting v_0/v_i versus $\sigma/(1 + \sigma)$ it is helpful to draw two ordinates: the first for $\sigma/(1 + \sigma) = 0$ and the second for $\sigma/(1 + \sigma) = 1$. For $[S] = K_m$, $\sigma/(1 + \sigma) = 0.5$ (Fig. 2.5a). Under the assumptions made above, linear or hyperbolic mechanisms of enzyme modification yield straight lines which have a common intersection with ordinate equal to 1 and abscissa corresponding to $(\alpha - \beta)/(\alpha - 1)$. The case $\alpha = 1$ with slope = 0 is the only exception to this rule. Otherwise the slope of the lines depends on the relationship between α and β as illustrated by the simulated examples in Fig. 2.6, where the modifier type can be recognized at a glance from the slope of the lines and the position of the abscissa intercept. For instance, inhibition types which are linear competitive or have a predominantly competitive component ($K_i < \alpha K_i$), the common intersection point lies on the right side of the plot. For calculating α , β and K_i the extrapolated intersections of the straight lines with the two ordinates are used. Defining ‘a’ the intersection with the left ordinate [$\sigma/(1 + \sigma) = 0$] and ‘b’ the intersection with the right ordinate [$\sigma/(1 + \sigma) = 1$], it follows from Eq. (2.9) that

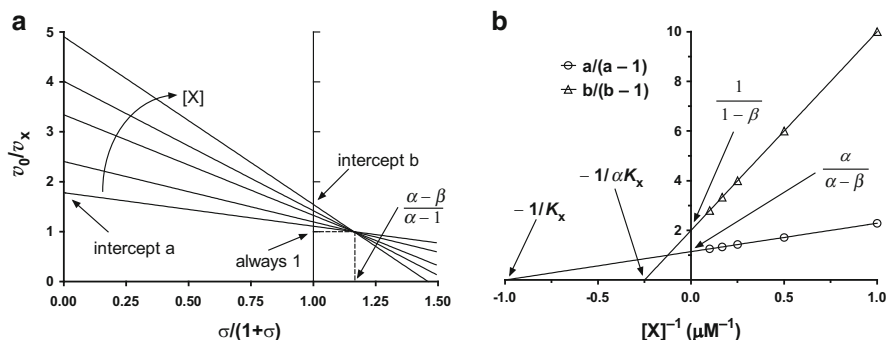


Fig. 2.5 Properties of the specific velocity plot illustrated with a simulated example of hyperbolic mixed inhibition. The primary and secondary plots are shown in panels (a) and (b), respectively. Independently of the mechanism (linear, mixed, inhibition or activation), with $\alpha \neq 1$ the family of straight lines in the primary plots intersect at a common point, with ordinate = 1 and abscissa = $(\alpha - \beta)/(\alpha - 1)$. As shown here, the primary and the secondary plot allow the calculation of the modifier equilibrium constant as well as of the α and β coefficients

$$a = \frac{1 + \frac{[X]}{K_x}}{1 + \frac{\beta[X]}{\alpha K_x}}; \quad b = \frac{1 + \frac{[X]}{\alpha K_x}}{1 + \frac{\beta[X]}{\alpha K_x}} \quad (2.10)$$

and straightforward rearrangement of these relationships yields

$$\frac{a}{a-1} = \frac{\alpha K_x}{\alpha - \beta} \frac{1}{[X]} + \frac{\alpha}{\alpha - \beta} \quad (2.11)$$

$$\frac{b}{b-1} = \frac{\alpha K_x}{1 - \beta} \frac{1}{[X]} + \frac{1}{1 - \beta}. \quad (2.12)$$

The plots of $a/(a-1)$ or $b/(b-1)$ versus $1/[X]$ are straight lines, from which α , β and K_i can be calculated (Fig. 2.5).

The simulated examples in Fig. 2.6 show the specific velocity plots and replots for linear competitive, linear mixed and hyperbolic mixed inhibition as well for non-essential activation.

The specific velocity plot is a plain graphical method for diagnostic purposes and for semiquantitative analysis of classical, reversible enzyme modification. The plot is superior to the double reciprocal plot in revealing subtle differences between competitive and mixed inhibitors and is therefore well suited for analyzing the action of allosteric effectors. We wish however to emphasize that this method is unsuitable for regression analysis. Namely, the ratio $\sigma/(1 + \sigma)$ is nothing else than v_0/V , which means that v_0 is part of the dependent as well as of the independent variable. This violates one of the fundamental principles of statistical methods for data analysis, i.e. that only the dependent variable is affected by errors (Sect. 2.4.3). Nevertheless, the specific velocity plot provides good estimates of inhibition or activation constants as well as the α and β

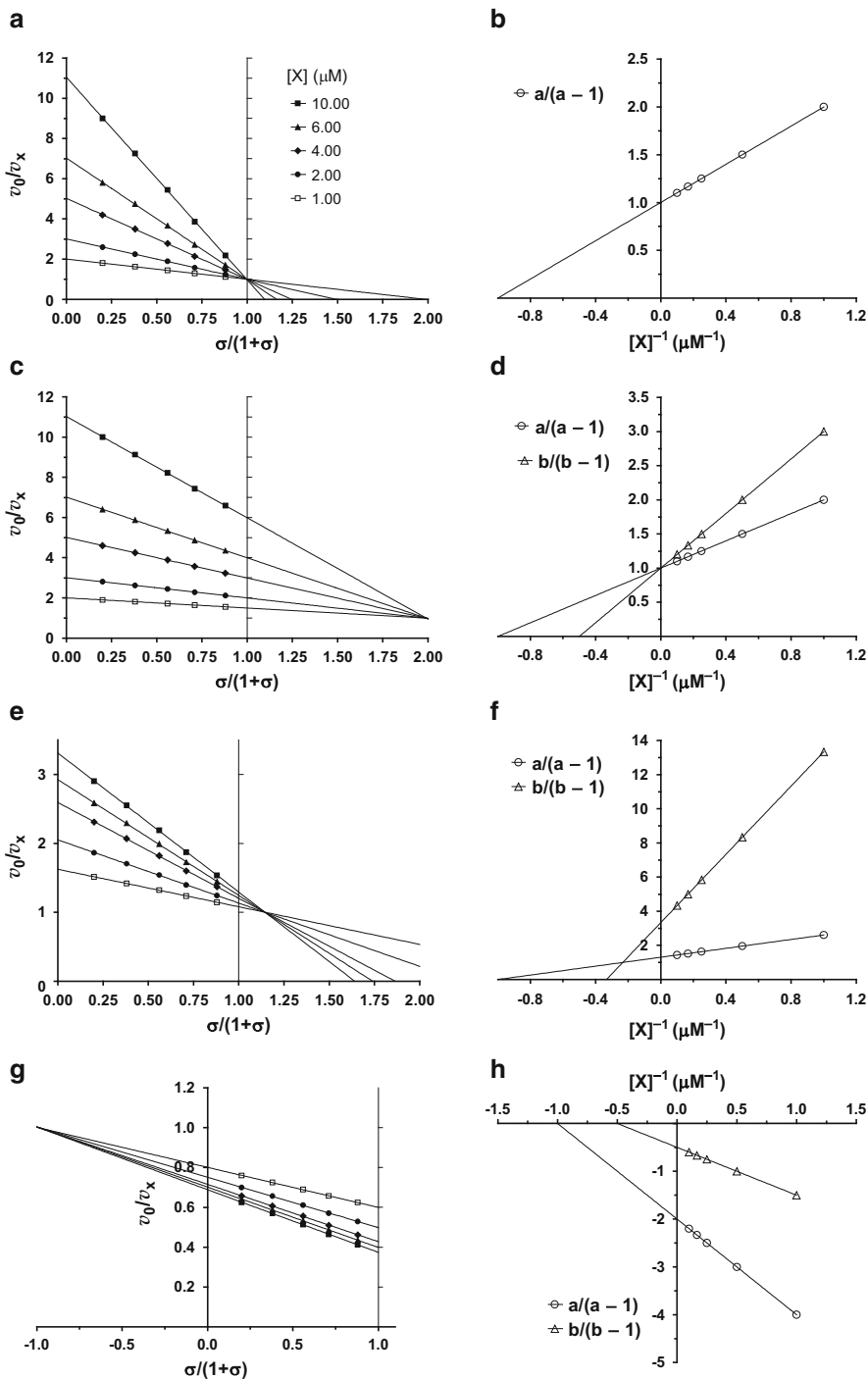


Fig. 2.6 Simulated examples of the specific velocity plot (a, c, e, g) and replots (b, d, f, h). The four examples were simulated with the following common parameters: $k_{\text{cat}} = 20 \text{ s}^{-1}$, $[E]_t = 0.025$

coefficients of the general modifier mechanism, which can be further used for refining calculations using Eq. (2.8) considering the modifier concentration as the independent variable.

2.6.3 A General Equation for Classical and Tight-Binding Systems

The treatment of the general modifier mechanism and of the specific velocity plot tacitly assumed that the concentration of free and total modifier was about the same ($[X] \approx [X]_t$) in every instance. Here we consider the case of tight inhibitor binding and examine first the relationships between $[I]_t$, $[E]_t$ and K_i . If comparable concentrations of enzyme and inhibitor give rise to appreciable inhibition and if this process is diffusion controlled, i.e. it occurs very rapidly, we are faced with tight-binding inhibition. This concept must be stated more precisely because it can for instance happen that, with 1 mM enzyme and inhibitor, full inhibition occurs because $K_i = 1 \mu\text{M}$. However, with inhibitor and enzyme at a concentration of 0.01 μM the degree of inhibition will be lower. The condition for tight-binding inhibition is therefore precisely defined with $[I]_t \approx [E]_t$ and K_i (Table 2.4).

A rate equation for tight-binding inhibition, valid for both linear and hyperbolic inhibition mechanisms, has been derived by Baici (1987). A regrettable error in this paper, which prevented the universal use of this equation for any mechanism, has been amended by Szedlacsek et al. (1988), who used symbols different from those of the original. To keep consistency with the symbols used in this chapter, the equation is written here using the same notation of the general modifier mechanism:

$$v_i = \frac{v_0}{2} \left[\frac{\alpha + \sigma - \beta(1 + \sigma)}{\alpha + \sigma} \right] \left\{ \sqrt{\left[\left(\frac{1 + \sigma \alpha K_i}{\alpha + \sigma [E]_t} + \frac{[I]_t}{[E]_t} - 1 \right)^2 + 4 \frac{1 + \sigma \alpha K_i}{\alpha + \sigma [E]_t} \right]} + \frac{\alpha + \sigma + \beta(1 + \sigma)}{\alpha + \sigma - \beta(1 + \sigma)} - \frac{1 + \sigma \alpha K_i}{\alpha + \sigma [E]_t} - \frac{[I]_t}{[E]_t} \right\}. \quad (2.13)$$

Equation (2.13), which contains the total concentrations of inhibitor and enzyme, can be used for calculating the inhibition constant of both classical and

Fig. 2.6 (continued) μM , from which $V = 0.5 \mu\text{M s}^{-1}$, $K_m = 20 \mu\text{M}$, $K_x = 1 \mu\text{M}$. Additionally: (a) and (b) (linear competitive inhibition) $\alpha = \infty$ and $\beta = 0$; (c) and (d) (linear mixed inhibition) $\alpha = 2$ and $\beta = 0$; (e) and (f) (hyperbolic mixed inhibition) $\alpha = 3$ and $\beta = 0.7$; (g) and (h) (non-essential activation) $\alpha = 2$ and $\beta = 3$. The same five inhibitor concentrations (μM) shown in panel (a) were used for all examples

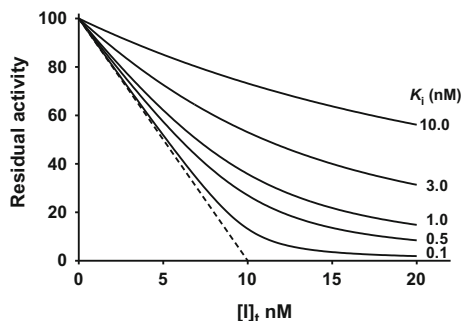


Fig. 2.7 Tight-binding inhibition. Simulated curves of residual activity versus total inhibitor concentration calculated with Eq. (2.13) and the following parameters: $v_0 = 100$, $\alpha = \infty$ (in practice a large value such as 10^9), $\beta = 0$, $\sigma = 1$, $[E]_t = 10$ nM, K_i five values (nM) as shown in the figure, $[I]_t$ continuously varied between 0 and 20 nM. The dashed line represents the titration curve, which can be obtained with an irreversible inhibitor

tight-binding inhibitors that may be linear or hyperbolic. It is indispensable whenever the concentrations of enzyme and inhibitor are in the same order of magnitude and the value of K_i prevents the validity of the assumption $[I] \approx [I]_t$. Precise calculations require of course the knowledge of the active sites concentration of the enzyme.

The relationship between $[I]_t$, $[E]_t$ and K_i is illustrated in Fig. 2.7, which shows residual activity profiles as a function of the total concentration of a linear competitive inhibitor at fixed enzyme concentration and variable K_i . Depending on the magnitude of the inhibition constant, the residual activity profile comes close to the titration curve, the dashed straight line in Fig. 2.7, which can be obtained with an irreversible inhibitor.

The properties of Fig. 2.7 can be exploited for determining the active concentration of a protein inhibitor of peptidases using an enzyme whose active sites concentration has been previously measured by titration with an irreversible inhibitor. This procedure is explained in Fig. 2.8 for a preparation of the human thyroglobulin type-1 domain of testican 3 (TST3) as a linear competitive inhibitor of human cathepsin B with a known $K_i = 13.6$ nM. The enzyme was previously titrated with the inactivator E-64 and used at a known final concentration in a further experiment with variable TST3 amounts, whose concentration as protein was known. The residual activity in the presence of a fluorogenic substrate and with a titrated cathepsin B concentration in the assays of 10.0 nM is plotted in Fig. 2.8 versus the total inhibitor concentration as protein, measured photometrically. It is immediately seen that any attempt at extrapolating the unknown TST3 concentration from the curve is useless (the ‘true’ titration line would correspond to the straight dashed line). Hence, Eq. (2.13) was fitted to data by treating the enzyme concentration as the sole parameter to be optimized, i.e. all parameters in the equation were set as known (see the legend of Fig. 2.8), while only $[E]_t$ was allowed to float during non-linear regression. The best fit value for $[E]_t$ was 13.0 ± 2.9 nM.

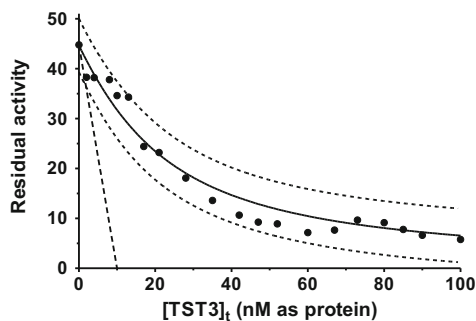


Fig. 2.8 Titration of human cathepsin B with known active site concentration with TST3 as reversible inhibitor. Residual activity (fluorescence reading units) plotted versus TST3 total concentration as protein. Equation (2.13) was fitted to data (black dots) with the following fixed parameters: $v_0 = 44.8$, $\alpha = 10^9$ and $\beta = 0$ (linear competitive inhibitor), $\sigma = 0.12$, $K_i = 13.6$ nM. The enzyme active site concentration was known (10.0 nM) but was considered as the sole parameter to be fitted with the purpose of measuring the unknown active site concentration of the inhibitor and the best fit (solid line) gave $[E]_t = 13.0 \pm 2.9$ nM. The dashed straight line indicates the titration curve that would be obtained with an irreversible inhibitor, and the dashed bent curves show the 95 % confidence band. The runs test suggested no significant deviation from the model

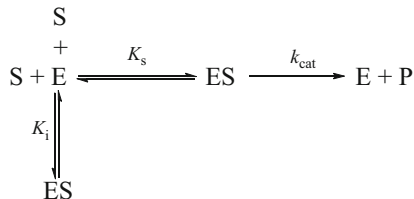
Since the true enzyme concentration was 10.0 nM, the protein concentration of TST3 was multiplied by the factor $10/13 = 0.77$ to obtain its active site concentration, i.e. the inhibitor preparation was 77 % active.

An example of kinetic analysis, in which the specific velocity plot for diagnostic purposes and of Eq. (2.13) for quantitative analysis were combined is the inhibition of caspase-2 by a designed ankyrin repeat. This modifier behaves as an allosteric effector of caspase-2 and acts as a hyperbolic mixed inhibitor. The kinetic mechanism fits neatly with the crystal structure of the complex (Schweizer et al. 2007).

2.6.4 Non-productive Binding and Substrate Inhibition

The substrates of peptidases are oligomers or large polymers. Apart the physiologically relevant cases of limited proteolysis, in which just one peptide bond is cleaved within a polypeptide, large protein substrates may be cleaved at multiple sites, i.e. wherever ‘specific’ susceptible bonds are recognized by the enzymes. For practical reasons, *in vitro* measurements are performed with synthetic oligopeptides of low molecular mass, which in virtue of their less bulky structure may be expected to bind the enzyme not only in the productive way leading to peptide bond cleavage, but possibly in one or more additional unproductive ways that do not lead to proteolytic breakdown. This situation can be described kinetically as shown in Scheme 2.7, which is analogous to linear competitive inhibition. If more than one non-specific binding site exists Scheme 2.7 symbolizes the average of all of them.

Scheme 2.7 Non-productive substrate binding



This inhibition is of the linear competitive type and its rate equation can be obtained from the general modifier mechanism, Eq. (2.8), by setting $\alpha = \infty$ and $\beta = 0$. The explicit expression $[\text{S}]/K_m$ for σ is used to clearly describe the properties of this system:

$$v = \frac{V[\text{S}]}{K_m \left(1 + \frac{[\text{S}]}{K_i} \right) + [\text{S}]} \quad (2.14)$$

The ‘substrate’ is thus at the same time substrate and inhibitor and there is no way to appreciate that inhibition exist from velocity measurements at various substrate concentrations because a rectangular hyperbola is obtained with or without such an inhibitory effect. Equation (2.14) can namely be rearranged to

$$v = \frac{\frac{V}{1 + \frac{K_m}{K_i}} [\text{S}]}{\frac{K_m}{1 + \frac{K_m}{K_i}} + [\text{S}]} \quad (2.15)$$

According to Cornish-Bowden (p. 137 in Cornish-Bowden 2004), calling \tilde{V} and \tilde{K}_m the parameters that would be observed in the absence of non-productive binding, Eq. (2.15) is equivalent to the Michaelis-Menten equation

$$v = \frac{V[\text{S}]}{K_m + [\text{S}]},$$

in which the limiting rate and the Michaelis constant are divided by the same factor

$$V = \frac{\tilde{V}}{1 + \frac{\tilde{K}_m}{K_i}}, \quad K_m = \frac{\tilde{K}_m}{1 + \frac{\tilde{K}_m}{K_i}} \quad (2.16)$$

The relevant aspect is that $V/K_m = \tilde{V}/\tilde{K}_m$ and thus the competitive inhibitory nature of substrates that bind non-productively will remain unobserved (see also Fig. 2.9). Therefore, the measured values of the kinetic parameters will be biased by an unknown factor with respect to parameters expected from the binding mode that

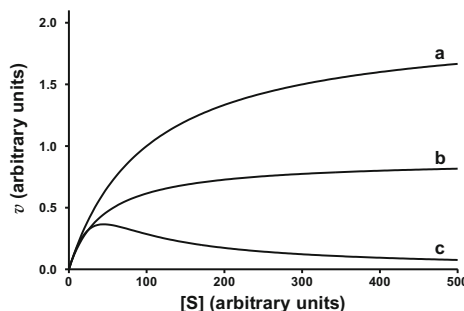
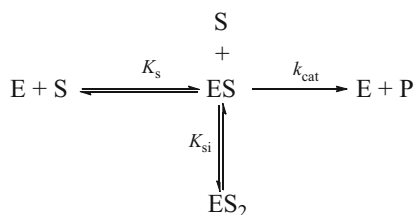


Fig. 2.9 Non-productive binding and substrate inhibition. The three curves were simulated with the common parameters $V = 2$ and $K_m = 100$. a—Michaelis-Menten equation (2.1); b—non-productive binding, Eq. (2.14), with $K_i = 80$; c—substrate inhibition, Eq. (2.17), with $K_{si} = 20$ (parameters and concentrations in arbitrary units)



Scheme 2.8 Uncompetitive substrate inhibition

results in peptide bond cleavage. This means that comparing k_{cat} , K_m and k_{cat}/K_m for different peptide substrates may not always reflect the authentic ‘specificity’ of the considered peptidase.

The term ‘substrate inhibition’ is reserved to the case in which a substrate molecule binds to an already formed ES complex according to the mechanism in Scheme 2.8.

Oligopeptide synthetic substrates of peptidases are very often involved in substrate inhibition of this type when substrate is in excess. The rate equation for this mechanism is deduced as a particular case of the general modifier mechanism, Eq. (2.8), with $\beta = 0$, $[S]$ replacing $[X]$, and αK_i called now K_{si} to indicate the inhibitory action of the substrate

$$v = \frac{V' [S]}{K'_m + [S] + \frac{[S]^2}{K_{si}}} \quad (2.17)$$

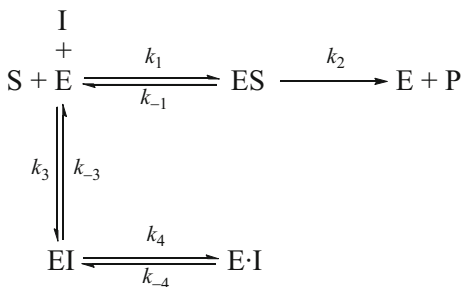
The primed symbols on limiting rate and Michaelis constant emphasize the fact that they cannot be considered Michaelis parameters because the rate has a limit of zero for $[S] \rightarrow \infty$, not V' , and K'_m does not correspond to the substrate concentration for which $v = V'/2$. In fact, the squared substrate concentration in the denominator of Eq. (2.17) forces the rate approaching zero at infinite $[S]$. Non-productive binding and

substrate inhibition are illustrated graphically in Fig. 2.9. In curve b it is shown that non-productive binding is characterized by a rectangular hyperbola, for which any inhibitory substrate effect cannot be suspected in the absence of additional information. Curve c describes substrate inhibition and curve a shows the ‘regular’ profile that would be obtained in the absence of any inhibitory effects.

2.7 Slow-Binding Inhibition

The nomenclature of the ‘slow’ mechanisms adopted here is that of Table 2.4. Chemical reasons for the slow inhibiting behavior include: (1) the formation of an intermediate with structural analogy to the transition state during catalysis; (2) fast binding of the inhibitor to the enzyme but true inhibition is only accomplished after slow rearrangement of the enzyme conformation; (3) a molecule exists in equilibrium between two or more chemical forms of which only one is the true inhibitor, which may have a small concentration so that the second-order association reaction $E + I \rightarrow EI$ may proceed very slowly; (4) the enzyme exists in two interconverting conformational states, of which only one binds the inhibitor. The kinetic information that can be extracted from slow-binding and slow, tight-binding inhibition experiments is larger than that obtained from conventional steady-state measurements of fast-acting inhibitors. In fact, besides overall inhibition constants, also second-order rate constants for the formation of the inhibited enzyme and rate constants for the dissociation of the E-I complex can be calculated. Two approaches are possible: to use the integrated rate equation for diagnosing the mechanism and calculating the parameters, or to simulate the process by numerical integration using all individual kinetic constants starting from initial guesses and then fitting iteratively the integrated progress curves to data by non-linear regression (Sect. 2.4.4). For slow-binding systems both methods have the own advantages and limitations. Integrated rate equations can only be derived under restrictive assumptions or cannot be derived at all, but provide valuable information about the underlying mechanism if the assumptions can be kept under control experimentally. Furthermore, the dependencies on $[I]$ of the parameters calculated by regression analysis represent a powerful diagnostic tool for model discrimination. Numerical integration does not depend on restrictive assumptions and can combine the information from different sets of experiments fitted globally to exploit the full statistical power of the method. Model discrimination can only be performed by running individually the relevant models with the same data and comparing the statistical outputs to find the best matching set. The major drawback of numerical integration is in many instances the large number of individual kinetic constants that must be fitted for some mechanisms and the impossibility of finding a unique array of constants that matches the model. In other words, despite superb mathematics, it is often impossible to decide which mechanism best describes the data and to evaluate all of the constants for the system because these are not well

Scheme 2.9 The general case of linear competitive, slow-binding inhibition



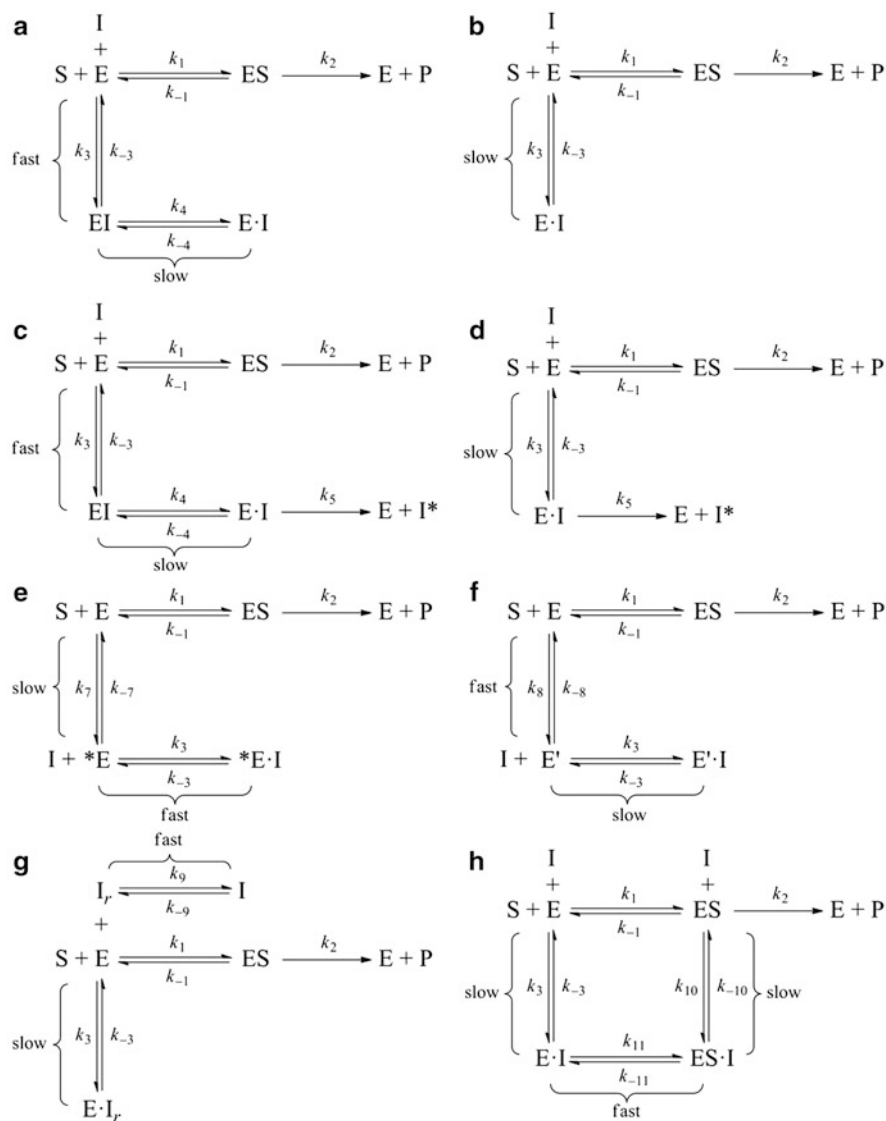
constrained by data. The two-step mechanism of linear competitive, slow-binding inhibition shown in Scheme 2.9 illustrates this problem.

Whenever a linear competitive inhibitor manifests slow-binding behavior and neither for the inhibitor nor for the enzyme, equilibria between different forms are known from chemical or other evidence, the mechanism in Scheme 2.9 should be considered first without making any assumption about the relative rates of equilibration of the two steps, the existence of only one step or any other simplifying aspect. The attainment of the steady-state for this mechanism is preceded by two exponential phases. Thus, the first logical approach is to fit the generic Eq. (2.18) (single exponential followed by a linear increase of the function) and Eq. (2.19) (double exponential followed by linear increase) to data and to determine which one fits the data better than the other. The *A*-factors in these equations are the amplitudes of the exponential phases and *d* is a displacement on the ordinate. It is anticipated that one of the two phases may be relatively rapid and/or may have a small amplitude. Thus, conventional methods for data acquisition may be inadequate because the time ‘lost’ for mixing solutions and activating the recording of reaction progress may take a relatively long time with loss of precious data. In such cases the use of a stopped-flow apparatus is highly recommended.

$$Y = A_1(1 - e^{-\lambda_1 t}) + kt + d \quad (2.18)$$

$$Y = A_1(1 - e^{-\lambda_1 t}) + A_2(1 - e^{-\lambda_2 t}) + kt + d \quad (2.19)$$

If it can be established that Eq. (2.18) fits the primary data (progress curves) better than Eq. (2.19), it can be assumed that one of the two steps of the mechanism in Scheme 2.9 is much more rapid than the other or that the mechanism degenerates to a single-step reaction between enzyme and inhibitor. The same reasoning holds for other mechanisms characterized by just one slow step and, correspondingly, the integrated equation for all these systems contains only one exponential phase. For these mechanisms, described in Sect. 2.7.1, an integrated rate equation can be obtained. For the general case shown in Scheme 2.9 an integrated rate equation has been derived under restrictive conditions, but due to its complexity it can hardly be used in practice (Kuzmič 2008). However, this and any other slow-binding mechanism can be analyzed by numerical integration as described with an example in Sect. 2.7.3.



Scheme 2.10 Mechanisms for slow-binding inhibition of peptidases. The numbering of kinetic constants is consistently kept throughout the mechanisms to identify the same or similar paths

2.7.1 Integrated Rate Equations: Their Usefulness and Limits

A common trend in the literature has been to consider the two mechanisms shown in panels (a) and (b) of Scheme 2.10 as the major representatives of slow-binding inhibition systems. While these might really be the most frequently encountered

mechanisms, in most instances analysis was conducted on the assumption of an underlying linear competitive mechanism without demonstrating this fact by adequate experiments. In principle, any other of the mechanisms shown in Scheme 2.10 may be responsible for the sluggishness of the inhibition process, a matter of fact that must be considered.

For all mechanisms in Scheme 2.10 (but see the comments below on the temporary inhibition mechanisms c and d) the integrated rate equation is given by

$$[P] = v_s t - \frac{(v_s - v_z)}{\lambda} (1 - e^{-\lambda t}) + d, \quad (2.20)$$

where v_s and v_z are the velocities at steady-state and at time zero, respectively, λ is an apparent first-order constant that describes the exponential phase, and d a displacement on the ordinate of the progress curve that accounts for any non-zero value of the signal proportional to $[P]$ at the beginning of the reaction, e.g. absorbance or fluorescence of the substrate before hydrolysis of the susceptible peptide bond. This equation has originally been published by Frieden in the context of enzyme hysteresis (Frieden 1970). The derivation of Eq. (2.20) is subordinated to the following restrictive assumptions: (1) steady-state conditions are set up very rapidly for the flux around E and ES; (2) non-steady state conditions exist for the steps marked 'slow' and rapid equilibrium conditions exist for the steps marked 'fast' in Scheme 2.10; (3) $[S]_t \gg [E]_t$ so that there is no depletion of free substrate through binding to the enzyme; (4) measurements are performed for a time that does not involve substantial turnover of substrate and accumulation of product; (5) $[I]_t$ is at least 10 times greater than $[E]_t$, meaning that the condition $[I] \approx [I]_t$ is valid throughout and tight-binding is not present.

With reference to Scheme 2.10, mechanism b is simply a degenerated form of mechanism a because the concentration of the EI complex is kinetically insignificant. Mechanisms c and d represent temporary inhibition, in which the E-I complex breaks down to free enzyme that is put back to bind substrate and inhibitor, and to an inactive form of the inhibitor I^* , in general a proteolytically cleaved form. We wish to emphasize that the integrated rate equation (2.20) for mechanisms c and d is valid only under the additional restrictive assumption that the decay of E-I into $E + I^*$ is a slow process and that $[I^*]$ remains much smaller than $[I]_t$ during the observation time of the experiment. This means that the inhibitor is present at a sufficiently high concentration, which acts as a sink to satisfy also the conditions $[I] \approx [I]_t$ and $[I]_t \gg [E]_t$. A safe experimental judgment for this condition is that the steady-state line represented by the straight line in trace b of Fig. 2.10 does not yet start to bend up (see below). Mechanism d has been demonstrated for instance in the reaction of cathepsin L with the thyroglobulin type-1 domain of human testican (Meh et al. 2005). Mechanisms e and f, in which the inhibitor binds to a rare form of the enzyme that fluctuates between two conformational states, are very similar and differ only for the position of the slow step. Mechanism e has been put forward in a non-proteolytic context (Duggleby et al. 1982) and mechanism f has been discussed in the frame of thermolysin inhibition by phosphonates (Bartlett and Marlowe

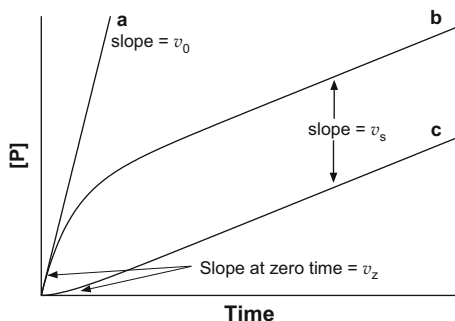


Fig. 2.10 Progress curves for slow-binding inhibition according to Eq. (2.20). a—enzyme incubated with substrate alone; b—reaction started by adding enzyme to a mixture of substrate and inhibitor; c—reaction started by adding substrate to enzyme preincubated with inhibitor for a sufficiently long time to allow formation of the inhibited complex

1987). Following the observation that peptidases may be present in different conformational states with distinct kinetic properties, e.g. cathepsin K at pH = 7.40 (Novinec et al. 2010), these two mechanisms should be included among the candidates in slow inhibition processes of peptidases.

In mechanism g the enzyme reacts with a rare form of the inhibitor (I_r), which exists in equilibrium with other species (Bartlett and Marlowe 1987). An example for peptidases is the inhibition of cathepsin B by leupeptin, which equilibrates between the free aldehyde, the aldehyde hydrate and a cyclic carbinolamine. Only the aldehyde form, which makes up merely 2 % of the total leupeptin concentration, is inhibitory. Thus, the slow-binding behavior of leupeptin is due to the low concentration of the inhibitor, which lowers the rate of E-I formation, and to the stability of an intermediate tetrahedral hemithioacetal (Schultz et al. 1989). Finally, mechanism h represents a linear, slow-binding mixed inhibition type, which has been demonstrated for adenosine deaminase (Cha 1976). This mechanism should be considered methodically when studying slow inhibition of peptidases, in particular by allosteric effectors.

Progress curves, as product concentration versus time conforming to the integrated equation (2.20), are shown in Fig. 2.10. In trace (b), in which reaction is started by adding enzyme to a mixture of substrate and inhibitor, slow inhibition is characterized by an exponential phase that is followed by a linear steady-state with slope v_s . This is the standard type of progress curves normally seen in the literature. Trace c in Fig. 2.10 results when enzyme and inhibitor are preincubated at high concentration to allow complex formation and reaction is started by diluting this mixture into a substrate-containing solution. The slopes of traces b and c are the same. The type of experiment as in trace c gives direct information on the dissociation constant of the inhibited complex and is precious for model discrimination. The slopes of traces b and c will not remain linear during the entire course of the reaction but will result in a horizontal plateau when all substrate has been used up. For the temporary inhibition mechanisms c and d in Scheme 2.10 the slope of

Table 2.6 Expressions of the parameters in Eq. (2.20) for mechanisms a and b in Scheme 2.10

Mechanism a	Mechanism b
$\lambda = k_{-4} + \frac{k_4[I]}{K_i \left(1 + \frac{[S]}{K_m} \right) + [I]} \quad (2.21)$	$\lambda = k_{-3} + \frac{k_3[I]}{1 + \frac{[S]}{K_m}} \quad (2.22)$
$K_i = \frac{k_{-3}}{k_3}$	
$v_z = \frac{V[S]}{K_m \left(1 + \frac{[I]}{K_i} \right) + [S]} \quad (2.23)$	$v_z = v_0 = \frac{V[S]}{K_m + [S]} \quad (2.24)$
$v_s = \frac{V[S]}{K_m \left(1 + \frac{[I]}{K_i^*} \right) + [S]} \quad (2.25)$	$v_s = \frac{V[S]}{K_m \left(1 + \frac{[I]}{K_i} \right) + [S]} \quad (2.26)$
$K_i^* = K_i \left(\frac{k_{-4}}{k_4 + k_{-4}} \right)$	

The expressions of v_z and v_0 apply to assays in which the reaction is started by adding enzyme to a solution containing substrate and inhibitor

trace b first slowly increases to a level equal to v_0 (trace a) and then declines to zero following substrate depletion. The form of trace c depends on the time the enzyme had been preincubated with inhibitor before adding substrate to start recording the proteolytic reaction. Of course, the proportion of degraded inhibitor I^* will increase with preincubation time and the form of the progress curves will vary. This experiment with temporary reversible inhibitors has thus no quantitative value but is highly diagnostic to detect temporary inhibition since in the extreme case of a very long preincubation, adding substrate will result in no inhibition with a slope corresponding to trace a, provided the enzyme has not lost activity for some reason during the incubation time.

While the various mechanisms have the same common integrated rate equation (2.20), what distinguishes them from one another are the expressions of v_s , v_z , and λ . These expressions, distributed in a number of specialized papers and reviews, are summarized below for practical consultation: Tables 2.6 and 2.7 list λ , v_z and v_s for mechanisms a–d of Scheme 2.10, while Table 2.8 lists only the values of λ for mechanisms e–h. If the assumptions made above for deriving Eq. (2.20) can be guaranteed experimentally and data are collected with precision, discrimination of the mechanisms in Scheme 2.10 can be accomplished by analyzing the dependency of v_s , v_z and λ on $[I]$. The relevant equations for these variables are then used to extract kinetic constants. The distinction between mechanisms a and b is straightforward because λ depends hyperbolically on $[I]$ in mechanism a and linearly in mechanism b, and v_z depends on $[I]$ in mechanism a, while it is independent of $[I]$ in mechanism b. The discrimination of mechanisms a and b from their corresponding temporary inhibition mechanisms c and d cannot be made on the basis of the

Table 2.7 Expressions of the parameters in Eq. (2.20) for the temporary inhibition mechanisms c and d in Scheme 2.10

Mechanism c	Mechanism d
$\lambda = k_{-4} + k_5 + \frac{k_4[I]}{K_i \left(1 + \frac{[S]}{K_m} \right) + [I]} \quad (2.27)$	$\lambda = k_{-3} + k_5 + \frac{k_3 K_m}{K_m + [S]} [I] \quad (2.28)$
$K_i = \frac{k_{-3}}{k_3}$	
$v_z, \text{ the same as Eq. (2.23)}$	$v_z, \text{ the same as Eq. (2.24)}$
$v_s = \frac{V[S]}{K_m \left\{ 1 + \frac{[I]}{K_{i, \text{temp}}^*} \right\} + [S]} \quad (2.29)$	$v_s = \frac{V[S]}{K_m \left(1 + \frac{[I]}{K_{i, \text{temp}}} \right) + [S]} \quad (2.30)$
$K_{i, \text{temp}}^* = K_i \frac{k_{-4} + k_5}{k_4 + k_{-4} + k_5}$	$K_{i, \text{temp}} = \frac{k_{-3} + k_5}{k_3}$

The expressions of v_z and v_0 apply to assays in which the reaction is started by adding enzyme to a solution containing substrate and inhibitor. These equations are only valid under the assumption $[I^*] \ll [I]_t$

Table 2.8 Expressions for λ in Eq. (2.20) for mechanisms e, f, g, and h in Scheme 2.10

Mechanism e	Mechanism f
$\lambda = \frac{k_7}{1 + \frac{[S]}{K_m}} + \frac{k_{-7}}{1 + \frac{[I]}{K_i}} \quad (2.31)$	$\lambda = k_{-3} + k_3 \frac{K_e [I]}{1 + K_e + \frac{[S]}{K_m}} \quad (2.32)$
	$K_e = \frac{[E']}{[E]}$
Mechanism g	Mechanism h
$\lambda = k_{-3} + k_3 \frac{K_r [I]}{1 + \frac{[S]}{K_m}} \quad (2.33)$	$\lambda = \frac{k_{-3} + \frac{k_{-10} k_{11}}{k_{-11}} [S]}{1 + \frac{k_{11}}{k_{-11}} [S]} + \frac{k_3 + k_{10} \frac{[S]}{K_m}}{1 + \frac{[S]}{K_m}} [I] \quad (2.34)$
$K_r = \frac{[I_r]}{[I]} \ll 1$	

dependencies of v_s , v_z and λ upon $[I]$ because the shape of the functions are the same, but they can readily be distinguished from one another by preincubating enzyme and inhibitor for increasing times and starting reactions by adding substrate (trace c in Fig. 2.10). The slope of the steady-state portion of the curve will be independent of the preincubation time for mechanisms a and b but will increase with incubation time for mechanisms c and d as a consequence of inhibitor degradation to I^* . Mechanism e poses no diagnostic problems because it is the only one for which λ depends hyperbolically on $[I]$ but in the reverse direction, i.e. decreasing for increasing $[I]$. Furthermore, for mechanism e, the asymptote of λ for $[I] \rightarrow \infty$ equals $k_7/(1 + [S]/K_m)$ and thus depends on substrate concentration.

In the other mechanisms for which λ has a hyperbolic dependence on $[I]$ (mechanisms a and c), λ increases for increasing $[I]$ and the asymptote is independent on $[S]$. More puzzling is the diagnosis of mechanisms f, g and h on the basis of the dependence of λ upon $[I]$, which is linear as it is for mechanisms b and d. However, the slopes of the steady-state lines of progress curves will reveal the mixed-type nature of mechanism h, which can then be diagnosed and the constants determined. As a general comment, the vast majority of publications on slow-binding inhibition report progress curves measured at a fixed enzyme and substrate concentration and variable $[I]$. However, it would be very useful to perform the same experiments also keeping $[I]$ constant for variable $[S]$ in order to determine if the inhibitor has a competitive or a mixed character. Finally, mechanisms f and g cannot be diagnosed on the basis of kinetics alone since they would be mostly ascribed to mechanism b. This shows that any information about enzyme properties, in particular the existence of interconverting enzyme conformations, should be considered. An example of how to recognize enzyme conformers is the already mentioned work on cathepsin K (Novinec et al. 2010).

For space reasons we cannot show here graphical examples of the mechanisms of slow-binding inhibition discussed in this section. The reader might find useful a review of diagnostic methods for slow reversible and irreversible inhibition (Baici et al. 2009).

2.7.2 *Slow, Tight-Binding Inhibition*

When the condition $[I] \approx [I]_t$ cannot be met Eq. (2.20) is not usable and the inhibition is of the tight-binding type. Integrating the rate equation for such systems is not always possible. Out of the mechanisms in Scheme 2.10, integrated rate equations for the tight-binding condition have been published for case b (Cha 1980; Williams et al. 1979) and for case h (Cha 1976), while for mechanism a and for its more general counterpart shown in Scheme 2.9 analytical integration is not possible. In any case, the integrated rate equations for slow, tight-binding are subjected to restrictive assumptions. These equations are not reproduced here because the method described below in Sect. 2.7.3 is free of such limitations and supersedes analytical integration.

2.7.3 *Numerical Integration Coupled to Non-linear Regression*

When an integrated rate equation can either not be obtained or the assumptions/conditions listed in Sect. 2.7.1 cannot be realized experimentally, or if tight-binding further complicates the situation, numerical integration is the method of choice for

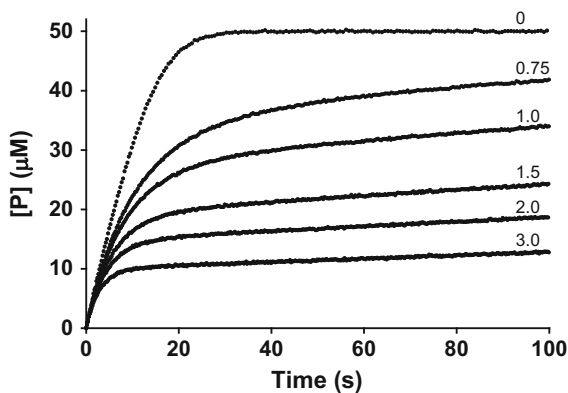


Fig. 2.11 Simulated data for slow, tight-binding inhibition. The simulation was performed with Simulink software using the following kinetic constants and total concentrations: $k_1 = 100 \mu\text{M}^{-1} \text{s}^{-1}$, $k_{-1} = 1,990 \text{s}^{-1}$, $k_2 = 10 \text{s}^{-1}$ (these constants give $K_m = 20 \mu\text{M}$), $k_3 = 0.4 \mu\text{M}^{-1} \text{s}^{-1}$, $k_{-3} = 0.003 \text{s}^{-1}$, $[\text{E}]_t = 0.5 \mu\text{M}$, $[\text{S}]_t = 50 \mu\text{M}$. Numbers next to the curves represent $[\text{I}]_t$ in μM units

data analysis. The best way to illustrate this method is to work out an example. We deal here with mechanism b in Scheme 2.10 for which a set of ‘data’ was simulated with Simulink as shown in Fig. 2.11. Some noise was also added to the simulated curves to mimic a real experiment. In this example we assume that the enzyme is not particularly stable in diluted solution over the period of 10–30 min typically necessary to measure slow-binding inhibition reactions. To overcome this problem experiments can be performed using a high enzyme concentration in order to shorten the reaction time and the progress curves are conveniently measured with a stopped-flow apparatus (less than 2 min in Fig. 2.11). The details of the kinetic constants and initial reactant concentrations are described in the figure legend. Since $[\text{E}]_t = 0.5 \mu\text{M}$, with the kinetic constants of the system we have also tight-binding, meaning that a considerable portion of the added inhibitor binds to the enzyme and the condition $[\text{I}] \approx [\text{I}]_t$ is invalid. Figure 2.11 shows that during reaction, depending on inhibitor concentration, 20–80 % of substrate is converted to product. Thus, with both inhibitor and substrate depletion, the integrated rate equation cannot be used neither in the form of Eq. (2.20) nor in the specially adapted form for slow, tight-binding inhibition (Cha 1980; Williams et al. 1979). Despite this fact, we compare now the results that can be obtained with the ‘illegal’ use of Eq. (2.20) with those from numerical integration. We start by fitting Eq. (2.20) to the data of Fig. 2.11 as shown in Fig. 2.12. Judging from the good superimposition of the fitted curves and data we could conclude that the fitting procedure is successful, but let us examine the values of the kinetic constants that we can extract from this procedure. The fit gives v_s , v_z and λ , from which the kinetic constants can be obtained from a plot of λ versus the inhibitor concentration (Fig. 2.13, see also Eq. (2.22) for λ in Table 2.6, mechanism b). The values of the kinetic constants are shown in Fig. 2.13 and summarized in Table 2.9 for comparison with the error-free data and with the method of numerical integration.

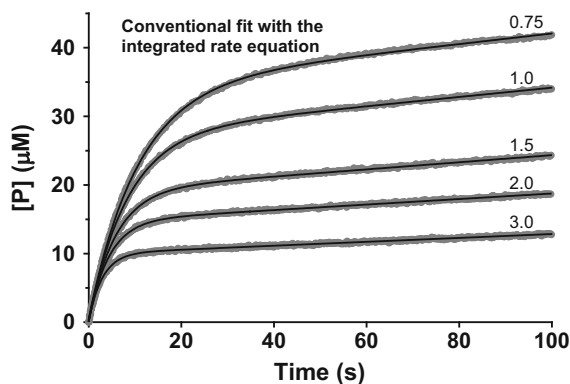


Fig. 2.12 Fit of Eq. (2.20) to the data in Fig. 2.11 using the five curves in the presence of inhibitor. The values of λ obtained for each inhibitor concentration are used to extract kinetic constants (Fig. 2.13). Numbers next to the curves represent $[I]_i$ in μM units. *Thick, noisy traces* represent data and *thin continuous lines* best fit curves

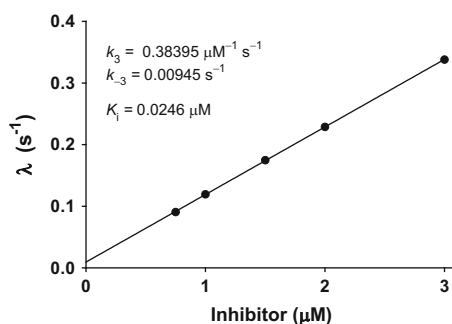


Fig. 2.13 Calculation of kinetic constants using the values of λ obtained from the best fit in Fig. 2.12. According to the equations for mechanism b in Table 2.6, k_3 and k_{-3} can be calculated from the slope and intercept of the *straight line*, respectively. $K_i = k_{-3}/k_3$

We evaluate now the same rate constants by numerical integration using KinTek software. The fitted curves, which include the control curve in the absence of inhibitor, are shown in Fig. 2.14. The quality of the fit was ascertained by calculating the confidence contours from globally fitting all progress curves. A limited range of mutual dependence of k_3 and k_{-3} indicated that these constants were determined precisely and were well constrained by the data. Kinetic constants with associated errors are summarized in Table 2.9.

We see from this example the basic difference between conventional fitting by non-linear regression using integrated rate equations (Table 2.9 method B) and fitting by numerical integration (Table 2.9 method C). Comparing the rate constants calculated by non-linear regression or by numerical integration with the reference values (Table 2.9 method A) we see that the rate constant k_3 is estimated fairly well

Table 2.9 Kinetic constants and error analysis for the example of slow-, tight-binding inhibition (primary data in Fig. 2.11)

Methods and properties	k_3 ($\mu\text{M}^{-1} \text{s}^{-1}$)	k_{-3} (s^{-1})	$K_i = k_{-3}/k_3$ (nM)
(A) Error-free values simulated with Simulink	0.4	0.003	7.5
(B) Integrated rate equation			
Best fit	0.38395	0.00945	24.6
Standard error	0.00165	0.00086	2.2
95 % confidence intervals	0.3787–0.3892	0.0067–0.0122	
(C) Numerical integration			
Best fit	0.3995	0.002973	7.44
Standard error	4.27×10^{-4}	7.69×10^{-5}	0.19
95 % confidence intervals	0.397–0.402	0.00285–0.00312	

All decimals from calculations are shown for the parameters to compare the precision of the methods

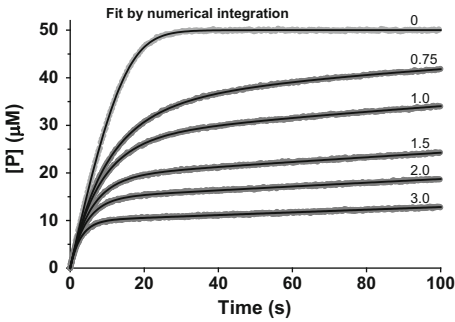
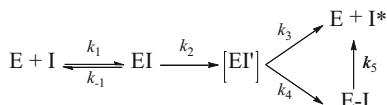


Fig. 2.14 Global fit of all curves in Fig. 2.11, including the curve with substrate alone, by numerical integration using KinTek software. Numbers next to the curves represent $[I]_t$ in μM units. *Thick, noisy traces* represent data and *thin continuous lines* best fit curves

by non-linear fitting and very good by numerical integration. On the contrary, the estimate of the rate constant k_{-3} by non-linear regression is poor, whereas we obtain a value very close to the true one by numerical integration. This discrepancy is clearly seen in the value of K_i , which is overestimated by the ‘illegal’ method B (24.6 nM), while numerical integration gives a satisfactory estimate of 7.44 nM. The small deviations of method C with respect to error free values (A) are due to the noise introduced in the curves.

2.7.4 The Serpin Inhibition Mechanism

Serpins are a superfamily of peptidase inhibitors found in a variety of organisms ranging from human to plants and viruses and share a unique mechanism of action. They inhibit mostly serine peptidases, from which the name ‘serpin’ derives

Scheme 2.11 The serpin inhibition mechanism

(SERine Peptidase INhibitors), while some also exhibit cross-class inhibition, e.g. the serpin CrmA inhibits granzyme B as well as caspases (Komiyama et al. 1994). The serpin molecule can exist in multiple conformations of which only one has inhibitory activity. In this canonical conformation, the ‘reactive center loop’, which is the main determinant of inhibitory activity and specificity, is exposed on the top of the serpin molecule and can interact with the active site of its target.

Serpins behave as mechanism-based (suicide) inhibitors that act by trapping the target enzyme in a covalent, essentially irreversible, enzyme-inhibitor complex. The major role in target recognition is performed by the reactive center loop which hence determines the specificity of each serpin. The basic kinetic mechanism of serpin inhibition is shown in Scheme 2.11. First, an adsorptive non-covalent EI complex is formed by insertion of the reactive center loop into the peptidase active site. From here the reaction proceeds analogous to a substrate cleavage reaction through a tetrahedral intermediate to the formation of an acyl-enzyme complex EI' with an overall rate constant k_2 . At this point the reaction can either proceed with rate constant k_3 to yield cleaved serpin I* and recycled enzyme, or the EI' complex can rearrange with rate constant k_4 to a kinetically trapped, covalently bound E-I complex. E-I can further break down into free enzyme and cleaved serpin in a slow process with rate constant k_5 .

Considering that k_5 is much smaller than k_3 , the ratio of serpin molecules needed to inhibit one enzyme molecule is defined as the stoichiometry of inhibition (SI)

$$SI = \frac{k_3 + k_4}{k_4}. \quad (2.35)$$

The value of SI depends on the ratio between k_3 and k_4 and can theoretically take any value larger than or equal to 1. Experimentally, SI values are determined from the ratio between cleaved serpin and stable, covalent E-I complex, though caution is advised in these experiments due to the high sensitivity of the SI to experimental conditions *in vitro*, such as ionic strength, temperature, pH, etc. The rate of complex formation can be determined from kinetic assays using low molecular mass synthetic substrates. However, one must take into account that the overall reaction rate of covalent complex formation (enzyme inactivation) includes both pathways in the mechanism. Hence, we can only measure an apparent overall association rate constant k_{app} , which is defined as

$$k_{app} = \frac{k_2}{K_m} \frac{1}{SI}, \quad (2.36)$$

with k_2 as overall rate constant for the formation of the acyl-enzyme complex, which is the rate-limiting step in the mechanism, and K_m is the Michaelis constant

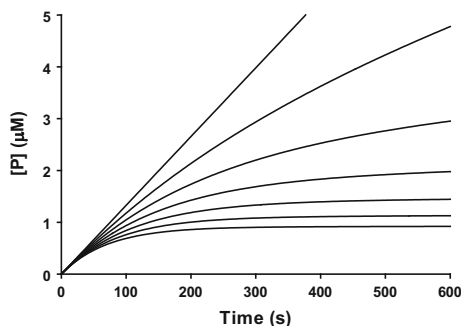


Fig. 2.15 Simulation of progress curves for the inhibition of human elastase-2 (EC 3.4.21.37) by wild-type α 1-peptidase inhibitor. The simulation was performed with KinTek software with 1.0 nM enzyme and 500 μ M MeOSuc-AAPV-p-nitroanilide as substrate. Published values of kinetic parameters were: $k_{\text{app}} = 1.2 \times 10^7 \text{ M}^{-1} \text{ s}^{-1}$ (Hopkins et al. 1993), $k_{\text{cat}} = 17 \text{ s}^{-1}$ and $K_{\text{m}} = 0.14 \text{ mM}$ (Nakajima et al. 1979). Inhibitor concentrations were 0, 1, 2, 3, 4, 5 and 6 nM from top to bottom

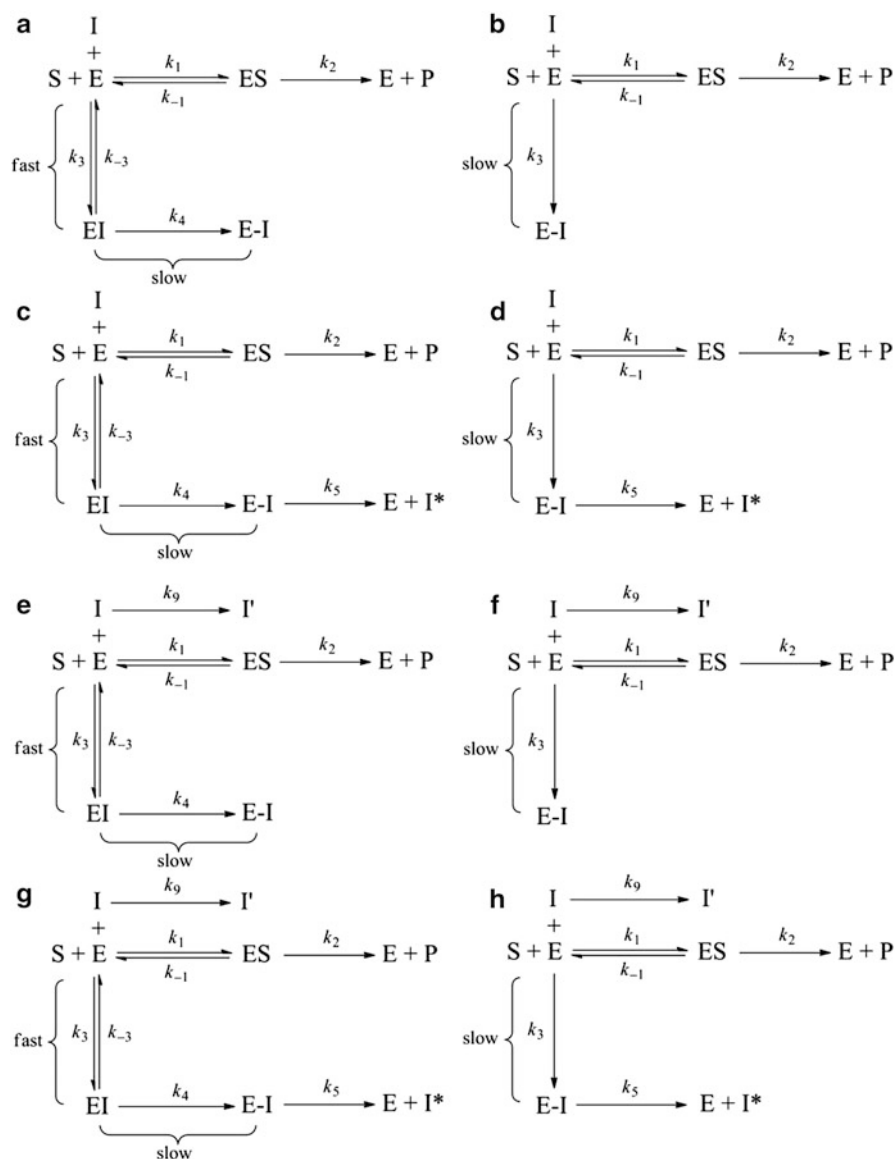
for the reaction with the substrate used to monitor reaction. A simulated example of progress curves typically obtained in such experiments is shown in Fig. 2.15.

2.8 Enzyme Inactivation

Enzyme inactivation results from the (mostly) slow reaction of irreversible modifiers with catalytically essential elements of enzymes. The covalent compound formed in the reaction is called here E-I to allow identification towards a reversible E-I complex at a glance. Examples are the inactivation of serine peptidases by diisopropyl fluorophosphate and the inactivation of cysteine peptidases by the *trans*-epoxysuccinic acid derivative E-64. The kinetic treatment of enzyme inactivation is the same as that of slow-binding inhibition with the difference that E-I does not dissociate back to its components. Representative examples of inactivation mechanisms relevant to peptidases are shown in Scheme 2.12, where the numbering of paths, where applicable, was kept in line with the corresponding reversible mechanisms in Scheme 2.10. Mechanisms a–d in Scheme 2.12 match the reversible counterparts with the same identification labels. The lack of reversibility in the reaction between E and I and the absence of a steady-state phase simplifies the integrated rate equation for mechanisms a and b to

$$[P] = \frac{v_z}{\lambda} (1 - e^{-\lambda t}) + d, \quad (2.37)$$

where v_z , λ and d have the same meaning as in Eq. (2.20). For the temporary inactivation mechanisms c and d the integrated rate equation must consider enzyme recycling, which results in continuously re-feeding the flux around E and ES. The integrated rate equation for mechanisms c and d is given by



Scheme 2.12 Mechanisms for enzyme inactivation relevant to peptidases. The numbering of kinetic constants is consistently kept throughout the mechanisms to identify the same or similar paths and to match numbering in Scheme 2.10

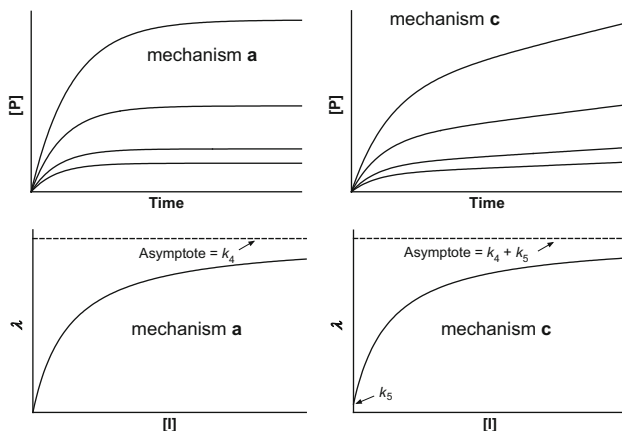


Fig. 2.16 Progress curves and the dependency of λ on inactivator concentration for mechanisms a and c in Scheme 2.12, as indicated

Table 2.10 Expressions of the parameters in Eq. (2.37) for mechanisms a and b in Scheme 2.12

Mechanism a	Mechanism b	
$\lambda = \frac{k_4[I]}{K_i \left(1 + \frac{[S]}{K_m} \right) + [I]}$	$\lambda = \frac{k_3[I]}{1 + \frac{[S]}{K_m}}$	(2.40)
$K_i = \frac{k_{-3}}{k_3}; \quad k_i = \frac{k_4}{K_i}$		

v_z , the same as Eq. (2.23)

v_z , the same as Eq. (2.24)

It is implicitly intended that reactions are started by adding enzyme to a solution containing substrate and inhibitor. k_3 and $k_i = k_4/K_i$, with units $M^{-1} s^{-1}$, are second-order constant of enzyme inactivation in mechanisms a and b, respectively, used to report enzyme inactivation results

$$[P] = v_\infty t + \frac{v_z - v_\infty}{\lambda} (1 - e^{-\lambda t}) + d, \quad (2.38)$$

in which v_∞ substitutes v_s of the reversible counterpart (Baici et al. 2009). v_∞ has the meaning of a velocity at the end of the exponential phase, which is obtained mathematically by setting $t = \infty$ in $e^{-\lambda t}$. Typical progress curves for mechanism a and its temporary counterpart c of Scheme 2.12, together with the dependencies of λ on $[I]$ are shown in Fig. 2.16. The expressions of v_∞ , v_z and λ for mechanisms a, b and c, d are shown in Tables 2.10 and 2.11, respectively.

While the diagnosis of mechanism a is straightforward for the hyperbolic dependence of λ on $[I]$ and the curve starting at the origin of the coordinates, which makes a distinction from the other mechanisms, temporary inactivation mechanism c is characterized by progress curves that cannot be distinguished from reversible slow-binding inhibition. A practical way for distinguishing

Table 2.11 Expressions of the parameters in Eq. (2.38) for mechanisms c and d in Scheme 2.12

Mechanism c	Mechanism d
$\lambda = k_5 + \frac{k_4[I]}{K_i \left(1 + \frac{[S]}{K_m}\right) + [I]} \quad (2.42)$	$\lambda = k_5 + \frac{k_3[I]}{1 + \frac{[S]}{K_m}} \quad (2.43)$
$K_i = \frac{k_{-3}}{k_3}$	
$v_z, \text{ the same as Eq. (2.23)}$	$v_z, \text{ the same as Eq. (2.24)}$
$v_\infty = \frac{V[S]}{K_m \left\{1 + \frac{[I]}{K_i} \left(1 + \frac{k_4}{k_5}\right)\right\} + [S]} \quad (2.44)$	$v_\infty = \frac{V[S]}{K_m \left(1 + \frac{k_3}{k_5} [I]\right) + [S]} \quad (2.45)$

Reactions started by adding enzyme to a solution containing substrate and inhibitor

mechanism c in Scheme 2.12 from slow-binding inhibition mechanism a in Scheme 2.10 is to preincubate enzyme and inactivator and to start reaction by adding substrate. The steady-state slope is independent of preincubation time for the reversible mechanism but does depend on time in temporary inactivation.

The one-step inactivation mechanism b is characterized by a linear dependence of λ on $[I]$ with the line passing through the origin of the coordinates, as suggested by Eq. (2.40). The distinction of the temporary inactivation mechanism d from slow-binding inhibition in one step (mechanism b in Scheme 2.10) is again possible by preincubating enzyme with inactivator and starting reaction with substrate.

Low molecular mass compounds designed as irreversible inhibitors of peptidases may occasionally undergo non-enzymatic degradation in the assay solution, e.g. by hydrolysis to an inactive molecule. This fact, described by mechanisms e and f in Scheme 2.12, must be taken into account in the calculation of kinetic constants. To further complicate the picture, it may happen that an inactivator molecule undergoes spontaneous decomposition and is at the same time temporary as shown by mechanisms g and h. While molecules exhibiting the properties of these two last mechanisms can hardly have a practical value as inactivators of peptidases, and the labor involved in determining all constants may result in a mere academic exercise, the experimenter must be prepared to recognize this possibility.

For mechanisms e–h in Scheme 2.12 integrated equations can either not be derived or are exceedingly complex and hence the method of choice for elucidating their kinetic behavior is to go straight to numerical integration with the method illustrated in Sect. 2.7.3. Yet, *Topham* developed a method for mechanisms e and f, which may be felt knotty by less experienced end users, but is nevertheless very useful (*Topham 1990*). For instance, the following integrated rate equation obtained by Maclaurin series expansion, has been successfully applied to acetylcholinesterase inactivators acting with mechanism f in Scheme 2.12 (*Baici et al. 2009*):

$$[P] = \frac{v_z}{k_9} e^{-\left\{ \frac{k_3 K_m [I]_t}{k_9 (K_m + [S])} \right\}} \left\{ k_9 t + \sum_{i=1}^{\infty} \left\{ \frac{k_3 K_m [I]_t}{k_9 (K_m + [S])} \right\}^i \frac{[1 - (e^{-k_9 t})^i]}{i \cdot i!} \right\}. \quad (2.41)$$

In Eq. (2.41) $v_z = v_0$ and the second-order inactivation constant k_3 , as well the first-order decay constant k_9 of the unstable inactivator, can be evaluated by non-linear regression. The number of terms in the Maclaurin series expansion depends on the value of k_9 ; with k_9 as small as 0.001 s^{-1} expansion to the tenth term is required, while the third term is sufficient for $k_9 = 0.005 \text{ s}^{-1}$.

Details on enzyme inactivation, with analysis and diagnostics of mechanisms accompanied by real kinetic measurements for most of the mechanisms in Scheme 2.12 have been published for a series of inactivators of acetylcholinesterase (Baici et al. 2009). As a warning for the reader, in this paper the indices of some kinetic constants differ from those in this chapter.

2.9 Further Concepts Relevant to Peptidases

2.9.1 Measuring ‘Invisible’ Kinetic Parameters

To investigate the interaction between peptidases and macromolecular substrates devoid of measurable signals for following reaction development, a progress curve method can be of help (Baici 1990). The macromolecular substrates can either be soluble proteins or even insoluble components of the extracellular matrix. The principle is based on incubating the enzyme with a synthetic fluorogenic substrate, the *reporter substrate*, in the presence of the macromolecular soluble substrate or finely powdered insoluble substrate such as elastin. With insoluble substrates the progress curves resemble those in the presence of slow-binding inhibitors and the information that can be extracted from the measurements are the mechanism and the rates of adsorption and desorption of the enzyme to/from the insoluble substrate, as studied e.g. with elastase-2 (Baici 1990) and the cathepsins K, L and S (Novinec et al. 2007). With soluble proteins substrates, the macromolecules can be formally treated as being competitive inhibitors but the ‘inhibition constant’ measured corresponds to K_m of the most susceptible peptide bond (Baici 1990). With this method, kinetic constants for the adsorption of cathepsins K, L and S to elastins from three different sources have been calculated with models similar to those used in interfacial enzyme catalysis, with the surface area of the insoluble substrate replacing concentrations (Novinec et al. 2007). This approach is also very useful to assess the action of peptidase inhibitors in presence of naturally occurring protein substrates and the physiological significance of these interactions, which pose serious problems to the pharmacological control of extracellular matrix-degrading peptidases (Baici 1998).

2.9.2 Double Enzyme-Modifier Interactions

The characterization of enzyme modifiers *in vitro*, either inhibitors or activators, starts with the analysis of the behavior of one modifier in presence of the target enzyme and a suitable substrate. However, *in vivo* it is conceivable that exogenous modifiers, e.g. therapeutically active inhibitors, may compete with endogenous inhibitors or other molecules capable of interacting with the enzyme. We developed a rigorous mathematical model to describe the behavior of inhibitors and activators in multiple-interaction systems (Schenker and Baici 2009). A general kinetic equation can describe apparently different phenomena ranging from inhibition to activation in any of 126 combinations of two enzyme modifiers. Paradoxical or otherwise unpredictable effects resulting from the action of two modifiers on the same enzyme can be analyzed and modeled with this general method.

2.9.3 Reporting Kinetic Results as IC_{50}

In reporting results of enzyme inactivation the useful parameter is the second-order inactivation constant (units $M^{-1} s^{-1}$), which corresponds to k_3 in the one-step mechanisms and to $k_i = k_4/K_i$ in the two-step mechanisms (Sect. 2.8). IC_{50} , the concentration of a *reversible* inhibitor at which v_0 is reduced by 50 %, depends on the inhibition type (Chou 1974; Naqui 1983). If applied *correctly*, IC_{50} can be used for reporting results (Cortés et al. 2001). However, IC_{50} to characterize *irreversible* inhibition does not make sense. Unfortunately, the ‘potency’ of irreversible inhibitors is often reported in the literature as IC_{50} . Enzyme inactivation is a time-dependent phenomenon: allowing *sufficient time* for the formation of E-I, enzyme activity is driven to zero if $[I]_t \geq [E]_t$. The reaction velocity corresponds to $\frac{1}{2}v_0$ only when $[I]_t = \frac{1}{2}[E]_t$. Thus, for enzyme inactivators, IC_{50} corresponds to one half the enzyme concentration used in the assay and has no further physical meaning.

References

- Auld DS (2004) Catalytic mechanisms for metallopeptidases. In: Barrett AJ, Rawlings ND, Woessner JF Jr (eds) Aspartic and metallo peptidases, vol 1, Handbook of proteolytic enzymes. Elsevier, London, pp 268–289
- Baici A (1981) The specific velocity plot. A graphical method for determining inhibition parameters for both linear and hyperbolic enzyme inhibitors. Eur J Biochem 119:9–14
- Baici A (1987) Graphical and statistical analysis of hyperbolic, tight-binding inhibition. Biochem J 244:793–796
- Baici A (1990) Interaction of human leukocyte elastase with soluble and insoluble protein substrates. A practical kinetic approach. Biochim Biophys Acta 1040:355–364
- Baici A (1998) Inhibition of extracellular matrix-degrading endopeptidases: problems, comments, and hypotheses. Biol Chem 379:1007–1018

- Baici A, Knöpfel M, Fehr K, Skvaril F, Böni A (1980) Kinetics of the different susceptibility of the four human immunoglobulin G subclasses to proteolysis by human lysosomal elastase. *Scand J Immunol* 12:41–50
- Baici A, Schenker P, Wächter M, Rüedi P (2009) 3-Fluoro-2,4-dioxa-3-phosphadecalins as inhibitors of acetylcholinesterase. A reappraisal of kinetic mechanisms and diagnostic methods. *Chem Biodivers* 6:261–282
- Bartlett PA, Marlowe CK (1987) Possible role for water dissociation in the slow binding of phosphorus-containing transition-state-analogue inhibitors of thermolysin. *Biochemistry* 26:8553–8561
- Botts J, Morales M (1953) Analytical description of the effects of modifiers and of enzyme multivalency upon the steady state catalyzed reaction rate. *Trans Faraday Soc* 49:696–707
- Cha S (1976) Tight-binding inhibitors—III. A new approach for the determination of competition between tight-binding inhibitors and substrates. Inhibition of adenosine deaminase by cofomycin. *Biochem Pharmacol* 25:2695–2702
- Cha S (1980) Tight-binding inhibitors—VII. Extended interpretation of the rate equation. Experimental designs and statistical methods. *Biochem Pharmacol* 29:1779–1789
- Chou T (1974) Relationships between inhibition constants and fractional inhibition in enzyme-catalyzed reactions with different numbers of reactants, different reaction mechanisms, and different types and mechanisms of inhibition. *Mol Pharmacol* 10:235–247
- Cleland WW (1963) The kinetics of enzyme-catalyzed reactions with two or more substrates or products. I. Nomenclature and rate equations. *Biochim Biophys Acta* 67:104–136
- Cornish-Bowden A (2004) Fundamentals of enzyme kinetics. Portland Press, London
- Cornish-Bowden A, Eisenthal R (1974) Statistical considerations in the estimation of enzyme kinetic parameters by the direct linear plot and other methods. *Biochem J* 139:721–730
- Cornish-Bowden A, Eisenthal R (1978) Estimation of Michaelis constants and maximum velocity from the direct linear plot. *Biochim Biophys Acta* 523:268–272
- Cornish-Bowden A, Porter WR, Trager WF (1978) Evaluation of distribution-free confidence limits for enzyme kinetic parameters. *J Theor Biol* 74:163–175
- Cortés A, Cascante M, Cárdenas ML, Cornish-Bowden A (2001) Relationships between inhibition constants, inhibitor concentrations for 50% inhibition and types of inhibition: new ways of analysing data. *Biochem J* 357:263–268
- Duggleby RG, Attwood PV, Wallace JC, Keech DB (1982) Avidin is a slow-binding inhibitor of pyruvate carboxylase. *Biochemistry* 21:3364–3370
- Eisenthal R, Cornish-Bowden A (1974) The direct linear plot. A new graphical procedure for estimating enzyme kinetic parameters. *Biochem J* 139:715–720
- Eisenthal R, Danson MJ, Hough DW (2007) Catalytic efficiency and k_{cat}/K_M : a useful comparator? *Trends Biotechnol* 25:247–249
- Fenner G (1931) Das Genauigkeitsmass von Summen, Differenzen, Produkten und Quotienten der Beobachtungsreihen. *Naturwissenschaften* 19:310
- Fersht A (1977) Enzyme structure and mechanism. Freeman, New York
- Fontes R, Ribeiro JM, Sillero A (2000) Inhibition and activation of enzymes. The effect of a modifier on the reaction rate and on kinetic parameters. *Acta Biochim Pol* 47:233–257
- Frieden C (1970) Kinetic aspects of regulation of metabolic processes. The hysteretic enzyme concept. *J Biol Chem* 245:5788–5799
- Hopkins PCR, Carrell RW, Stone SR (1993) Effects of mutations in the hinge region of serpins. *Biochemistry* 32:7650–7657
- International Union of Biochemistry (1979) Units of enzyme activity. *Eur J Biochem* 97:319–320
- International Union of Biochemistry (1982) Symbolism and terminology in enzyme kinetics. Recommendations 1981. *Eur J Biochem* 128:281–291
- James MNG (2004) Catalytic pathway of aspartic peptidases. In: Barrett AJ, Rawlings ND, Woessner JF Jr (eds) Aspartic and metallo peptidases, vol 1, Handbook of proteolytic enzymes. Elsevier, London, pp 12–19
- Johansen G, Lumry R (1961) Statistical analysis of enzymic steady-state rate data. *C R Trav Lab Carlsberg* 32:185–214

- Johnson KA (2009) Fitting enzyme kinetic data with Kintek Global Kinetic Explorer. *Methods Enzymol* 467:601–626
- Johnson KA, Simpson ZB, Blom T (2009a) FitSpace Explorer: an algorithm to evaluate multidimensional parameter space in fitting kinetic data. *Anal Biochem* 387:30–41
- Johnson KA, Simpson ZB, Blom T (2009b) Global Kinetic Explorer: a new computer program for dynamic simulation and fitting of kinetic data. *Anal Biochem* 387:20–29
- Komiyama T, Ray CA, Pickup DJ, Howard AD, Thornberry NA, Peterson EP, Salvesen G (1994) Inhibition of interleukin-1- β converting-enzyme by the cowpox virus serpin Crma. An example of cross-class inhibition. *J Biol Chem* 269:19331–19337
- Koshland DE (2002) The application and usefulness of the ratio k_{cat}/K_m . *Bioorg Chem* 30:211–213
- Kuzmič P (2008) A steady state mathematical model for stepwise “slow-binding” reversible enzyme inhibition. *Anal Biochem* 380:5–12
- Meh P, Pavšič M, Turk V, Baici A, Lenarčič B (2005) Dual concentration-dependent activity of thyroglobulin type-I domain of testican: specific inhibitor and substrate of cathepsin L. *Biol Chem* 386:75–83
- Morrison JF (1982) The slow-binding and slow, tight-binding inhibition of enzyme-catalysed reactions. *Trends Biochem Sci* 7:102–105
- Nakajima K, Powers JC, Ashe BM, Zimmerman M (1979) Mapping the extended substrate binding site of cathepsin G and human leukocyte elastase. Studies with peptide substrates related to the α 1-protease inhibitor reactive site. *J Biol Chem* 254:4027–4032
- Naqui A (1983) What does I50 mean? *Biochem J* 215:429–430
- Novinec M, Grass RN, Stark WJ, Turk V, Baici A, Lenarčič B (2007) Interaction between human cathepsins K, L and S and elastins: mechanism of elastinolysis and inhibition by macromolecular inhibitors. *J Biol Chem* 282:7893–7902
- Novinec M, Kovačič L, Lenarčič B, Baici A (2010) Conformational flexibility and allosteric regulation of cathepsin K. *Biochem J* 429:379–389
- Orsi BA, Tipton KF (1979) Kinetic analysis of progress curves. *Methods Enzymol* 63:159–183
- Polgár L (2004a) Catalytic mechanisms of cysteine peptidases. In: Barrett AJ, Rawlings ND, Woessner JF Jr (eds) *Cysteine, serine and threonine peptidases*, vol 2, *Handbook of proteolytic enzymes*. Elsevier, London, pp 1072–1079
- Polgár L (2004b) Catalytic mechanisms of serine and threonine peptidases. In: Barrett AJ, Rawlings ND, Woessner JF Jr (eds) *Cysteine, serine and threonine peptidases*, vol 2, *Handbook of proteolytic enzymes*. Elsevier, London, pp 1440–1448
- Rawlings ND, Barrett AJ, Bateman A (2010) MEROPS: the peptidase database. *Nucleic Acids Res* 38:D227–D233
- Schechter I, Berger A (1967) On the size of the active sites in proteases. I. Papain. *Biochem Biophys Res Commun* 27:157–162
- Schenker P, Baici A (2009) Simultaneous interaction of enzymes with two modifiers: reappraisal of kinetic models and new paradigms. *J Theor Biol* 261:318–329
- Schultz RM, Varma-Nelson P, Ortiz R, Kozłowski KA, Orawski AT, Pagast P, Frankfater A (1989) Active and inactive forms of the transition-state analog protease inhibitor leupeptin: explanation of the observed slow binding of leupeptin to cathepsin B and papain. *J Biol Chem* 264:1497–1507
- Schweizer A, Roschitzki-Voser H, Amstutz P, Briand C, Gulotti-Georgieva M, Prenosil E, Binz HK, Capitani G, Baici A, Plückthun A, Grütter MG (2007) Inhibition of caspase-2 by a designed ankyrin repeat protein: specificity, structure, and inhibition mechanism. *Structure* 15:625–636
- Segel IH (1975) *Enzyme kinetics. Behavior and analysis of rapid equilibrium and steady-state enzyme systems*. Wiley, New York
- Selwyn MJ (1965) A simple test for inactivation of an enzyme during assay. *Biochim Biophys Acta* 105:193–195
- Szedlacsek SE, Ostafe V, Serban M, Vlad MO (1988) A re-evaluation of the kinetic equations for hyperbolic tight-binding inhibition. *Biochem J* 254:311–312

- Tallant C, Marrero A, Gomis-Ruth FX (2010) Matrix metalloproteinases: fold and function of their catalytic domains. *Biochim Biophys Acta* 1803:20–28
- Topham CM (1990) A generalized theoretical treatment of the kinetics of an enzyme-catalysed reaction in the presence of an unstable irreversible modifier. *J Theor Biol* 145:547–572
- Williams JW, Morrison JF, Duggleby RG (1979) Methotrexate, a high-affinity pseudosubstrate of dihydrofolate reductase. *Biochemistry* 18:2567–2573

Proteases: Structure and Function

Brix, K.; Stöcker, W. (Eds.)

2013, XII, 564 p. 98 illus., 65 illus. in color., Hardcover

ISBN: 978-3-7091-0884-0